Computation of the Fourier transform for a continuous integrable function via NFFT

Daniel Potts* Manfred Tasche‡

July 28, 2026

We investigate the approximation of continuous Fourier transforms by trigonometric sampling polynomials and their efficient evaluation by the nonequispaced fast Fourier transform (NFFT). While the NFFT is traditionally used for the evaluation of trigonometric polynomials, we show that it can also serve as an effective computational tool for the approximation of Fourier transform values. Building on ideas of M. Ehler, K. Gröchenig, and A. Klotz [8], we derive explicit ℓ_∞ uniform error bounds between the Fourier transform and suitable sampling polynomials. The resulting estimates quantify the influence of the sampling width and truncation parameter and provide rigorous accuracy guarantees on entire frequency intervals. In contrast to previous analyses focusing mainly on discrete or L_2-type errors, our results yield uniform approximation bounds that are directly relevant for practical computations. Moreover, we prove a matching lower bound which shows that the derived rate in the truncation parameter is sharp.

The derived theory leads to a simple algorithmic framework: first approximate the Fourier transform by a trigonometric sampling polynomial and then evaluate this polynomial efficiently by the NFFT. Numerical experiments confirm the theoretical convergence rates and demonstrate that accurate approximations of continuous Fourier transforms can be obtained with moderate computational effort.

Key words: computation of Fourier transform, fast Fourier transform, nonequispaced fast Fourier transform, NFFT, maximum error estimates, Poisson summation formula, Wiener amalgam space.

AMS *Subject Classifications*: 42A38, 65T50, 94A20

*potts@math.tu-chemnitz.de, Chemnitz University of Technology, Faculty of Mathematics, D–09107 Chemnitz, Germany

‡manfred.tasche@math.uni-rostock.de, University of Rostock, Institute of Mathematics, D–18051 Rostock, Germany

1 Introduction

The nonequispaced fast Fourier transform (NFFT) is a well-established tool for the efficient evaluation of trigonometric polynomials at arbitrary nodes [7, 5, 28, 23, 12, 2]. Traditionally, the NFFT is employed once the Fourier coefficients of a trigonometric polynomial are already known. In many applications, however, the primary quantity of interest is not the trigonometric polynomial itself but the continuous Fourier transform

$$\hat{f}(v) = \int_{\mathbb{R}} f(x)\, \mathrm{e}^{-2\pi \mathrm{i}\, xv}\, \mathrm{d}x\,, \quad v \in \mathbb{R}\,, \tag{1.1}$$

This naturally raises the question whether the NFFT can also be used as a numerical method for computing values of the Fourier transform.

The present paper provides a positive answer to this question. Building upon ideas developed by M. Ehler, K. Gröchenig, and A. Klotz [8], we interpret trigonometric sampling polynomials as approximations of the Fourier transform and derive explicit uniform error estimates. These results show that the NFFT can be employed not only for the evaluation of trigonometric polynomials but also for the efficient computation of values of the continuous Fourier transform. Consequently, the NFFT becomes more than a fast evaluation scheme for trigonometric polynomials. Combined with the approximation results developed in this paper, it yields a practical and theoretically justified method for the computation of continuous Fourier transforms.

More precisely, we consider the computation of the Fourier transform of $\hat{f}$, see (1.1), under certain decay conditions on f and $\hat{f}$. We restrict f to the spatial domain $[-L/2,\, L/2]$ and $\hat{f}$ to the frequency domain $[-P/2,\, P/2]$, where $L \in 2\mathbb{N}$ and $P \in 2\mathbb{N}$ are sufficiently large positive integers. We sample f at the equispaced points j/P, $j \in [LP]$, with spatial step size $1/P$, where

$$[LP] := \big\{ j \in \mathbb{Z} : -\tfrac{LP}{2} < j \leq \tfrac{LP}{2} \big\}$$

denotes the centered index set. The *P-periodic trigonometric sampling polynomial of f with degree $LP/2$* is defined by

$$s_{P,L}(v) := \frac{1}{P} \sum_{n \in [LP]} f\Big(\frac{n}{P}\Big)\, \mathrm{e}^{-2\pi \mathrm{i}\, nv/P}\,, \quad v \in \mathbb{R}\,, \tag{1.2}$$

which approximates $\hat{f}(v)$ on the compact frequency interval $[-P/2,\, P/2]$. We determine approximate values of $\hat{f}\big(\frac{k}{L}\big)$, $k \in [LP]$, by evaluating the trigonometric sampling polynomial $s_{P,L}(v)$ at $v = k/L$, giving

$$s_{P,L}\big(\tfrac{k}{L}\big) = \frac{1}{P} \sum_{j \in [LP]} f\left(\frac{j}{P}\right) \mathrm{e}^{-2\pi \mathrm{i}\, jk/(LP)}\,, \quad k \in [LP]\,. \tag{1.3}$$

This standard approach to computing the Fourier transform is well documented in the literature (see, e.g., [6, pp. 17–23], [23, pp. 507–508], or [8]). Note that the values (1.3) can be computed efficiently via the fast Fourier transform (FFT), provided L and P are products of powers of the small primes, see [10]. More generally, the trigonometric

sampling polynomial $s_{P,L}(v)$ can be evaluated at arbitrary points v with $|v| \le P/2$ by means of the nonequispaced fast Fourier transform (NFFT). Recall that the NFFT is a fast approximate algorithm to evaluate a 1-periodic trigonometric polynomial

$$\sum_{k\in[M]} c_k \, \mathrm{e}^{2\pi \mathrm{i}\, kx}, \quad x \in \mathbb{R}, \tag{1.4}$$

with given coefficients $c_k \in \mathbb{C}$, $k \in [M]$, at given nonequispaced points $x_j \in [0, 1]$, $j = 1, \ldots, N$, where $M \in 2\mathbb{N}$. The fundamental idea of the NFFT is to exploit the FFT to efficiently switch between the spatial and frequency domains, thereby enabling a computationally efficient approximation at arbitrary nonuniform points. Throughout this paper, we assume that L, $P \in 2\mathbb{N}$ are sufficiently large.

In [8], M. Ehler, K. Gröchenig, and A. Klotz established error estimates for this computation of the values $\hat{f}\big(\frac{k}{L}\big)$ for $k \in [LP]$. Specifically, they studied how the scaled Euclidean approximation error

$$E^*_{P,L}(f) := \frac{1}{\sqrt{L}} \left(\sum_{k\in[LP]} \Big| \hat{f}\big(\tfrac{k}{L}\big) - s_{P,L}\big(\tfrac{k}{L}\big) \Big|^2 \right)^{1/2}$$

depends on P and L, given known decay behavior of $f \in C(\mathbb{R})$ and $\hat{f} \in C(\mathbb{R})$. These estimates are formulated in terms of norms of Wiener amalgam spaces [9].

In this paper, we address the analogous question for the scaled maximum approximation error

$$M_{P,L}(f) := \frac{1}{\sqrt{L}} \max_{|v|\le P/2} \big| \hat{f}(v) - s_{P,L}(v) \big|, \tag{1.5}$$

again under decay conditions on f and $\hat{f}$. In particular, we study the discretized version

$$M^*_{P,L}(f) := \frac{1}{\sqrt{L}} \max_{k\in[LP]} \Big| \hat{f}\big(\tfrac{k}{L}\big) - s_{P,L}\big(\tfrac{k}{L}\big) \Big| . \tag{1.6}$$

Obviously, it holds $M^*_{P,L}(f) \le M_{P,L}(f)$. Therefore we are interested in practicable, explicit upper bounds of $M_{P,L}(f)$. We discuss the following questions:

1. Under which decay assumptions on f and $\hat{f}$ can the Fourier transform $\hat{f}$ be uniformly approximated by the trigonometric sampling polynomial $s_{P,L}$ with explicitly controllable error?

2. How can the NFFT be employed to compute values of the continuous Fourier transform $\hat{f}(v)$ efficiently and with rigorous ℓ_∞ error bounds?

We introduce the so-called decay rate $\delta(f, L)$ of $f \in W(C(\mathbb{R}), \ell^1(\mathbb{Z}))$ with respect to step size $L \in 2\mathbb{N}$, which is defined by (3.2). If $f \in C(\mathbb{R})$ has polynomial or exponential decay (see Example 3.2), then the corresponding decay rate $\delta(f, L)$ can be easily estimated (see Lemma 3.9 and Lemma 3.15). Applying the Poisson summation formula (3.4), we show in Theorem 3.5 that an upper bound of $M_{P,L}(f)$ is a linear combination

of the decay rates $\delta(\hat{f}, P)$ and $\delta(f, L)$, if $f,\ \hat{f} \in W(C(\mathbb{R}), \ell^1(\mathbb{Z}))$ and $P,\ L \in 2\mathbb{N}$ are given.

Theorem 3.5 shows that the Fourier transform $\hat{f}$ can be approximated uniformly by the trigonometric sampling polynomial $s_{P,L}$ with an error controlled by the decay rates of f and $\hat{f}$. Since $s_{P,L}$ is a trigonometric polynomial, its values can be computed efficiently by FFT or NFFT techniques. Consequently, the theorem provides a rigorous foundation for the computation of continuous Fourier transforms by means of the NFFT.

The main contributions of this paper can be summarized as follows:

(C1) We introduce the decay rate $\delta(f, L)$ in (3.2) and prove in Theorem 3.5 the *uniform* error bound $M_{P,L}(f) \leq L^{-1/2}\,\delta(\hat{f}, P) + L^{1/2}\,\delta(f, L)$, valid on the whole interval $[-P/2,\ P/2]$ and not only on the grid $\{k/L\}$. This is the property which is needed if $s_{P,L}$ is evaluated at *arbitrary* nodes by the NFFT.

(C2) All constants in the resulting estimates (3.12), (3.15) and (3.16) are explicit and are computed directly from the decay parameters of f and $\hat{f}$. Moreover, the exponential case is treated for all $\alpha,\ \beta > 0$, whereas [8] is restricted to $0 < \alpha,\ \beta \leq 1$.

(C3) We prove in Theorem 3.20 a matching *lower* bound, which shows that the rate $L^{1/2-a}$ in the truncation parameter cannot be improved, and we determine in Remark 3.13 the exact range $\left[1,\ \sqrt{LP}\,\right]$ of the quotient $E^*_{P,L}(f)/M^*_{P,L}(f)$.

(C4) We state the resulting method explicitly as Algorithm 3.22, including its arithmetic cost and its a priori error bound, and we compare direct evaluation, FFT and NFFT numerically in Section 5.

This paper is organized as follows: Section 2 reviews the relevant literature and states precisely which of our results are new. In Section 3, we recall the Wiener amalgam space $W(C(\mathbb{R}), \ell^1(\mathbb{Z}))$, introduce the decay rate $\delta(f, L)$, and derive uniform error estimates for the scaled maximum approximation error $M_{P,L}(f)$ under polynomial, exponential, and mixed decay conditions on f and $\hat{f}$, together with a matching lower bound and the resulting Algorithm 3.22. Section 4 demonstrates how the theoretical error bounds translate into practical parameter choices for FFT- and NFFT-based approximations of the Fourier transform. In particular, the numerical experiments confirm that the NFFT yields highly accurate evaluations of $\hat{f}(v)$ throughout the frequency interval while preserving the expected computational efficiency. Section 5 is devoted to the computational cost and compares direct evaluation, FFT and NFFT. Section 6 concludes the paper.

2 Literature review

In this section we relate the present paper to the state of the art. We group the discussion into three strands – the approximation of the Fourier transform by discrete sums, the function-space framework, and fast algorithms – and close with a precise account of what is new here.

2.1 Approximation of the Fourier transform by discrete sums

Replacing the Fourier integral (1.1) by a finite sum of the form (1.3) is the oldest and most widely used numerical device in Fourier analysis; classical accounts are given in [6, pp. 17–23] and [23, pp. 507–508]. The two error sources – *aliasing*, caused by the discretization of the integral with step size $1/P$, and *truncation*, caused by restricting the sum to the window $[-L/2,\, L/2]$ – have long been understood qualitatively. Quantitative, non-asymptotic statements have been obtained only recently.

The paper of M. Ehler, K. Gröchenig, and A. Klotz [8] is the direct starting point of the present work. The authors measure the accuracy of (1.3) by the scaled Euclidean error $E^{*}_{P,L}(f)$ and prove, for f and $\hat{f}$ in Wiener amalgam spaces, bounds of the form $C\,(L^{-\alpha} + P^{-\beta})$ with $\alpha < a - \frac{1}{2}$ and $\beta < b - \frac{1}{2}$ in the case of polynomial decay, and of the form $C\,(\mathrm{e}^{-r'(L/2)^{\alpha}} + \mathrm{e}^{-s'(P/2)^{\beta}})$ with $r' < r$, $s' < s$ and $0 < \alpha,\, \beta \leq 1$ in the case of exponential decay. Their results are asymptotically sharp in the exponents, and they give an asymptotically optimal recipe for balancing the number of samples, the sampling step and the grid size. The loss in the exponents is intrinsic to their argument.

Closely related questions arise in the numerical realization of Shannon's sampling theorem, where a bandlimited function is reconstructed from finitely many samples. Sharp bounds for the norm of the Shannon sampling operator and regularized sampling formulas with sinh-type or continuous Kaiser–Bessel windows are studied in [18, 19]; see also the earlier work [27, 29]. These papers are concerned with the reconstruction of f from its samples, i.e. with the situation of Remark 3.6, whereas we are interested in the forward problem, the evaluation of $\hat{f}$.

2.2 The function-space framework

The natural setting for the Poisson summation formula (3.3)–(3.4) is the Wiener amalgam space $W(C(\mathbb{R}), \ell^1(\mathbb{Z}))$ introduced by N. Wiener [30, p. 73] and developed systematically by H.G. Feichtinger [9]; see also [14, pp. 103–105]. The example of Y. Katznelson [15] shows that the space $C(\mathbb{R}) \cap L^1(\mathbb{R})$ is genuinely too large, and K. Gröchenig [13] clarified the role of the underlying uncertainty principle. We adopt this framework unchanged from [8], since it is exactly the setting in which the two Poisson summation formulae hold pointwise and with absolute and uniform convergence, which is what a uniform error bound requires.

2.3 Fast algorithms

The NFFT goes back to A. Dutt and V. Rokhlin [7], G. Beylkin [5] and G. Steidl [28]; a survey is [12] and a textbook treatment is [23, Chapter 7]. Widely used software libraries are NFFT3 [16, 17] and FINUFFT [3, 2]; the experiments in Section 5 use the Python interface `pyNFFT3` [26] of NFFT3.

The accuracy of the NFFT itself – i.e. the error committed when the trigonometric polynomial (1.4) with *given* coefficients is evaluated approximately – is by now well understood. Uniform error estimates for compactly supported window functions are given

in [24], continuous window functions are analysed in [25], and the case of nonequispaced data in both domains, together with fast sinc transforms, is treated in [20]. The FINUFFT kernel is analysed in [4]. We stress that this line of work is complementary to ours: it bounds the difference between $s_{P,L}$ and its NFFT approximation, whereas we bound the difference between $\hat{f}$ and $s_{P,L}$. Only the combination of both, as in Algorithm 3.22 and Remark 3.23, yields a rigorous bound for the quantity a user actually computes.

2.4 What is new in this paper

Since the relation to [8] is close, we state explicitly which of our results are new, which cannot be obtained from [8], and which assumptions have been weakened. A synopsis is given in Table 2.1.

(N1) *A different, strictly finer error measure.* We estimate the maximum error $M_{P,L}(f)$ over the *whole interval* $[-P/2,\ P/2]$, while [8] estimates the Euclidean error $E^*_{P,L}(f)$ over the *finite grid* $\{k/L : k \in [LP]\}$. A maximum error does occur in [8, Section 2.7, formula (12)], but only through the trivial estimate $M^*_{P,L}(f) \le E^*_{P,L}(f)$, i.e. the discrete maximum error is bounded there by the Euclidean error and therefore inherits its rate. This is exactly the step which is lossy: the two quantities satisfy

$$M^*_{P,L}(f) \ \le\ E^*_{P,L}(f) \ \le\ \sqrt{LP}\, M^*_{P,L}(f)\,,$$

and both inequalities are attained up to constants, see Remark 3.13 and Figure 4.4b. The two error measures are therefore *not* equivalent: their quotient is unbounded as $LP \to \infty$. Consequently, Theorem 3.10 cannot be deduced from [8, Theorem 2.1] via [8, (12)]; that route yields only the exponent $P^{-b+1/2+\varepsilon}$ instead of P^{-b}, and the gap is clearly visible in Figure 4.4b. Conversely, an estimate on a finite grid carries no information about the values of $\hat{f} - s_{P,L}$ between the grid points, which is precisely the information needed when $s_{P,L}$ is evaluated by an NFFT at arbitrary nodes.

(N2) *Explicit constants.* All constants in (3.12), (3.15) and (3.16) are given in closed form in terms of the decay parameters a, b, c, d, r, s, α, β. This makes the estimates usable as an a priori stopping criterion, i.e. for the actual choice of L and P (see Algorithm 3.22).

(N3) *No loss in the exponents, and a weaker assumption in the exponential case.* In the polynomial case we obtain the exponent b in P and the exponent $a - \frac{1}{2}$ in L, whereas [8] must give away an arbitrarily small $\varepsilon > 0$ in both exponents. In the exponential case, [8, Theorems 2.3 and 2.4] assume $0 < \alpha,\ \beta \le 1$ and lose an arbitrarily small amount in the decay parameters r and s; Theorem 3.16 and Theorem 3.18 hold for *all* $\alpha,\ \beta > 0$ and retain the original r and s. In particular, the Gaussian ($\alpha = \beta = 2$) of Example 4.2 is not covered by [8].

(N4) *Sharpness.* Theorem 3.20 provides a lower bound which matches the upper bound of Theorem 3.10 in the truncation parameter L up to a constant factor. In [8] the

sharpness of the estimates is conjectured and confirmed by numerical experiments, but no lower bound is proved there.

(N5) *Algorithm and computational assessment.* Algorithm 3.22 combines the estimate of Theorem 3.5 with the NFFT and states the total error and the arithmetic cost; Section 5 compares direct evaluation, FFT and NFFT.

The general strategy of splitting the Poisson summation formula into a principal part and two remainders, and the use of Wiener amalgam spaces, are taken from [8], as is the scaling $L^{-1/2}$ in the definition (1.5) of the error, which we have kept in order to make the two sets of results directly comparable.

Table 2.1: Comparison of [8] with the present paper. Here a, $b > 1$ denote the polynomial and r, α, s, $\beta > 0$ the exponential decay parameters of f and $\hat{f}$; $\varepsilon > 0$ is arbitrarily small.

	[8]	this paper
error measure	$E^*_{P,L}(f)$, Euclidean, on the grid $\{k/L\}$; $M^*_{P,L}$ only via $M^*_{P,L} \le E^*_{P,L}$	$M_{P,L}(f)$, maximum, on all of $[-P/2, P/2]$
constants	not specified	explicit in $a, b, c, d, r, s, \alpha, \beta$
polynomial decay	$\mathcal{O}\big(L^{-a+1/2+\varepsilon} + P^{-b+1/2+\varepsilon}\big)$	$\mathcal{O}\big(L^{-a+1/2} + L^{-1/2}P^{-b}\big)$, Thm. 3.10
exponential decay	only $0 < \alpha, \beta \le 1$, rates $r' < r$, $s' < s$	all $\alpha, \beta > 0$, rates r, s, Thm. 3.16
lower bounds	conjectured, numerical evidence	proved, Thm. 3.20
evaluation at arbitrary v	not covered	Alg. 3.22, Rem. 3.23
cost comparison	–	Section 5

3 Uniform approximation by trigonometric sampling polynomials

The *Wiener amalgam space* $W(C(\mathbb{R}), \ell^1(\mathbb{Z}))$ is the Banach space consisting of all functions $f : \mathbb{R} \to \mathbb{C}$ which are *locally* in $C(\mathbb{R})$ and have *globally* an $\ell^1(\mathbb{Z})$ behavior at infinity in the sense that the uniform norms of f over the intervals $[k, k+1]$, $k \in \mathbb{Z}$, form a sequence in $\ell^1(\mathbb{Z})$. The norm of $W(C(\mathbb{R}), \ell^1(\mathbb{Z}))$ is given by

$$\|f\|_{W(C(\mathbb{R}),\ell^1(\mathbb{Z}))} := \sum_{k\in\mathbb{Z}} \max_{x\in[0,1]} |f(x+k)| .$$

The Wiener amalgam space was introduced by N. Wiener [30, p. 73] and was used as convenient function space in Fourier analysis, cf. [9], [14, pp. 103–105], and [8]. The condition $f \in W(C(\mathbb{R}), \ell^1(\mathbb{Z}))$ is strong enough to exclude many pathological functions which play a role in Fourier analysis but are of little practical interest. The Wiener amalgam space $W(C(\mathbb{R}), \ell^1(\mathbb{Z}))$ contains all continuous, compactly supported functions

and is therefore a dense subspace of the Lebesgue space $L^1(\mathbb{R})$. This Wiener amalgam space has the following property:

Lemma 3.1. (see [*14*, Lemma 6.1.2]) *If $f \in W(C(\mathbb{R}), \ell^1(\mathbb{Z}))$ and $R > 0$ are given, then*

$$\sup_{x\in\mathbb{R}} \sum_{k\in\mathbb{Z}} |f(x + Rk)| \leq \left(\frac{1}{R} + 1\right) \|f\|_{W(C(\mathbb{R}),\ell^1(\mathbb{Z}))} .$$

From Lemma 3.1 with $R = \frac{1}{L}$, $L \in 2\mathbb{N}$, it follows immediately that

$$\sum_{k\in\mathbb{Z}} \left|f\left(\tfrac{k}{L}\right)\right| \leq \left(\frac{1}{R} + 1\right) \|f\|_{W(C(\mathbb{R}),\ell^1(\mathbb{Z}))} < \infty \tag{3.1}$$

such that $\left(f\left(\frac{k}{L}\right)\right)_{k\in\mathbb{Z}} \in \ell^1(\mathbb{Z})$ for each $L \in 2\mathbb{N}$.

For each $f \in W(C(\mathbb{R}), \ell^1(\mathbb{Z}))$ we introduce the *decay rate of f with respect to the step size $L \in 2\mathbb{N}$* by

$$\delta(f, L) := \max_{|x|\leq L/2} \sum_{k\in\mathbb{Z}\setminus\{0\}} |f(x + kL)| . \tag{3.2}$$

From Lemma 3.1 it follows immediately that $\delta(f, L) < \infty$ for arbitrary $L \in 2\mathbb{N}$.

Example 3.2. *A function f belongs to the Wiener amalgam space $W(C(\mathbb{R}), \ell^1(\mathbb{Z}))$ if and only if $f \in C(\mathbb{R})$ can be majorized by the step function s with jumps at integers, given by $s(x) = m_k$ for $x \in [k, k + 1)$, $k \in \mathbb{Z}$, with $m_k := \max_{x\in[k,\,k+1]} |f(x)|$ and $\sum_{k\in\mathbb{Z}} m_k < \infty$. Hence it holds*

$$W(C(\mathbb{R}), \ell^1(\mathbb{Z})) \subset C(\mathbb{R}) \cap L^1(\mathbb{R}) .$$

In particular, each compactly supported function $f \in C(\mathbb{R})$ belongs to $W(C(\mathbb{R}), \ell^1(\mathbb{Z}))$. If $f \in C(\mathbb{R})$ has polynomial decay*, i.e.,*

$$\sup_{x\in\mathbb{R}} |f(x)| \, (1 + |x|)^a \leq c < \infty , \quad a > 1 ,$$

or exponential decay*, i.e.,*

$$\sup_{x\in\mathbb{R}} |f(x)| \, \mathrm{e}^{r\,|x|^\alpha} \leq d < \infty , \quad r, \alpha > 0 ,$$

then f belongs to $W(C(\mathbb{R}), \ell^1(\mathbb{Z}))$. For corresponding proofs see Lemma 3.9 and Lemma 3.15.

3.1 Poisson summation formula

The key tool for estimating the uniform approximation error is the Poisson summation formula. It allows us to express the error between $\hat{f}$ and the trigonometric sampling polynomial $s_{P,L}$ in terms of the tails of f and $\hat{f}$, which can then be controlled by decay conditions on these functions.

Lemma 3.3. (see [13]) *Let $P \in 2\mathbb{N}$ be fixed. For each $f \in W(C(\mathbb{R}), \ell^1(\mathbb{Z}))$ with $\hat{f} \in W(C(\mathbb{R}), \ell^1(\mathbb{Z}))$, the* Poisson summation formulae

$$\sum_{k\in\mathbb{Z}} f(x+kP) = \frac{1}{P}\sum_{n\in\mathbb{Z}} \hat{f}\Big(\frac{n}{P}\Big)\,\mathrm{e}^{2\pi\mathrm{i}\,nx/P}\,, \tag{3.3}$$

$$\sum_{k\in\mathbb{Z}} \hat{f}(v+kP) = \frac{1}{P}\sum_{n\in\mathbb{Z}} f\Big(\frac{n}{P}\Big)\,\mathrm{e}^{-2\pi\mathrm{i}\,nv/P} \tag{3.4}$$

hold for all x, $v \in \mathbb{R}$. All series converge absolutely and uniformly on $\mathbb{R}$.

Proof. From Lemma 3.1 it follows that

$$f_P(x) := \sum_{k\in\mathbb{Z}} f(x+kP)\,, \quad x \in \mathbb{R}\,,$$

is a continuous, P-periodic function. By the assumption $\hat{f} \in W(C(\mathbb{R}), \ell^1(\mathbb{Z}))$, it follows from (3.1) that

$$\sum_{k\in\mathbb{Z}} \Big|\hat{f}\Big(\frac{n}{P}\Big)\Big| < \infty\,,$$

so that the P-periodic Fourier series $\frac{1}{P}\sum_{n\in\mathbb{Z}} \hat{f}\big(\frac{n}{P}\big)\,\mathrm{e}^{2\pi\mathrm{i}\,nx/P}$ converges absolutely and uniformly on $\mathbb{R}$. Both functions coincide, since f_P has the P-periodic Fourier coefficients

$$\frac{1}{P}\int_0^P f_P(x)\,\mathrm{e}^{-2\pi\mathrm{i}\,nx/P}\,\mathrm{d}x = \frac{1}{P}\int_{\mathbb{R}} f(x)\,\mathrm{e}^{-2\pi\mathrm{i}\,nx/P}\,\mathrm{d}x = \frac{1}{P}\,\hat{f}\Big(\frac{n}{P}\Big)\,, \quad n \in \mathbb{Z}\,.$$

This completes the proof of (3.3). Replacing f by $\hat{f}$ yields (3.4). ■

Remark 3.4. *By an example, Y. Katznelson [15] has shown that the Poisson summation formula* (3.3) *does not hold for all $f \in C(\mathbb{R}) \cap L^1(\mathbb{R})$ with $\hat{f} \in C(\mathbb{R}) \cap L^1(\mathbb{R})$, illustrating the essential difference between the spaces $W(C(\mathbb{R}), \ell^1(\mathbb{Z}))$ and $C(\mathbb{R}) \cap L^1(\mathbb{R})$.*

3.2 The trigonometric sampling polynomial and its fast evaluation

The trigonometric sampling polynomial provides a natural approximation of the Fourier transform $\hat{f}$ on a compact frequency interval, and can be evaluated efficiently at arbitrary points using the NFFT. Now we make this precise.

For $f \in W(C(\mathbb{R}), \ell^1(\mathbb{Z}))$ with $\hat{f} \in W(C(\mathbb{R}), \ell^1(\mathbb{Z}))$ and sufficiently large L, $P \in 2\mathbb{N}$, we define the *P-periodic trigonometric sampling polynomial of f with sampling support $[-L/2, L/2]$ and degree $LP/2$* by $s_{P,L}$, see (1.2). Under suitable decay conditions on f and $\hat{f}$, the polynomial $s_{P,L}$ provides a good uniform approximation of $\hat{f}$ on the compact interval $[-P/2,\, P/2]$, see Theorem 3.5 and the following results.

The values $s_{P,L}(k/L)$, $k \in [LP]$, on the uniform frequency grid can be computed via the FFT in $\mathcal{O}(LP \log LP)$ operations, provided L and P are products of powers of small primes (see [10]). More generally, the trigonometric sampling polynomial $s_{P,L}$ can be

evaluated at K arbitrary points $v_1, \ldots, v_K \in [-P/2,\, P/2]$ by means of the nonequispaced fast Fourier transform (NFFT) in only $\mathcal{O}(LP \log LP + K)$ operations (see [23]). Hence, for each v with $|v| \le P/2$, the value $s_{P,L}(v)$ is a computationally efficient approximation of $\hat{f}(v)$.

3.3 The uniform approximation error

Let $L,\, P \in 2\mathbb{N}$ be given. By convenient decay conditions on f and $\hat{f}$, we can show that $s_{P,L}$ is a good uniform approximation of $\hat{f}$ on the compact interval $\left[-\frac{P}{2},\, \frac{P}{2}\right]$. To this end, we use the scaled uniform approximation error (1.5). If we form the maximum only on the grid $\left\{\frac{k}{L} : k \in [LP]\right\}$, then we obtain the discretized version of the scaled uniform approximation error (1.6). We derive explicit estimates for $M_{P,L}(f)$ and $M^*_{P,L}(f)$ under various decay conditions on f and $\hat{f}$. The key decomposition is provided by Theorem 3.5 below, which splits the error into two contributions: one governed by the decay of $\hat{f}$ and one by the decay of f. Explicit bounds for each contribution are then given in Lemma 3.9 and Lemma 3.15, covering the cases of polynomial and exponential decay respectively.

Theorem 3.5. *Let $L,\, P \in 2\mathbb{N}$ be fixed. Let $f \in W(C(\mathbb{R}), \ell^1(\mathbb{Z}))$ with $\hat{f} \in W(C(\mathbb{R}), \ell^1(\mathbb{Z}))$ be given.*
Then $\hat{f}$ can be uniformly approximated on $[-P/2, P/2]$ by the trigonometric sampling polynomial $s_{P,L}$, and it holds the estimate

$$M^*_{P,L}(f) \le M_{P,L}(f) \le \frac{1}{\sqrt{L}}\, \delta(\hat{f}, P) + \sqrt{L}\, \delta(f, L)\,, \tag{3.5}$$

where $\delta(\hat{f}, P)$ and $\delta(f, L)$ denote the corresponding decay rates (3.2).

Proof. Splitting both series in the second Poisson summation formula (3.4) into the principal terms and the remainders, we obtain for all $v \in \mathbb{R}$

$$\hat{f}(v) + \sigma_1(v) = s_{P,L}(v) + \sigma_2(v)\,,$$

with

$$\begin{aligned} \sigma_1(v) &:= \sum_{k \in \mathbb{Z}\setminus\{0\}} \hat{f}(v + kP)\,, \\ \sigma_2(v) &:= \frac{1}{P} \sum_{n \in \mathbb{Z}\setminus[LP]} f\Big(\frac{n}{P}\Big)\, \mathrm{e}^{-2\pi \mathrm{i}\, nv/P}\,. \end{aligned}$$

Hence this provides that

$$M^*_{P,L}(f) \le M_{P,L}(f) \le \frac{1}{\sqrt{L}} \max_{|v| \le P/2} |\sigma_1(v)| + \frac{1}{\sqrt{L}} \max_{|v| \le P/2} |\sigma_2(v)|\,.$$

Applying the triangle inequality and (3.2), we obtain

$$\max_{|v| \le P/2} |\sigma_1(v)| \le \max_{|v| \le P/2} \sum_{k \in \mathbb{Z}\setminus\{0\}} |\hat{f}(v + kP)| = \delta(\hat{f}, P)\,.$$

In the expression σ_2, the summation indices $n \in \mathbb{Z} \setminus [LP]$ can be written in the form $n = m + kLP$ with $m \in [LP]$ and $k \in \mathbb{Z} \setminus \{0\}$, such that

$$\sigma_2(v) = \frac{1}{P} \sum_{m \in [LP]} \sum_{k \in \mathbb{Z} \setminus \{0\}} f\Big(\frac{m}{P} + kL\Big)\, \mathrm{e}^{-2\pi \mathrm{i}\, mv/P}\, \mathrm{e}^{-2\pi \mathrm{i}\, kLv}\,.$$

Using triangle inequality and (3.2), this yields

$$\max_{|v| \le P/2} |\sigma_2(v)| \le \frac{LP}{P} \max_{m \in [LP]} \sum_{k \in \mathbb{Z} \setminus \{0\}} \Big| f\Big(\frac{m}{P} + kL\Big) \Big| \le L\, \delta(f, L)\,.$$

This completes the proof. ■

Remark 3.6. *For given f, $\hat{f} \in W(C(\mathbb{R}), \ell^1(\mathbb{Z}))$, we can analogously estimate the maximum approximation error*

$$\frac{1}{\sqrt{L}} \max_{|x| \le P/2} \left| f(x) - \frac{1}{P} \sum_{n \in [LP]} \hat{f}\Big(\frac{n}{P}\Big)\, \mathrm{e}^{2\pi \mathrm{i}\, nx/P} \right| \tag{3.6}$$

by applying the first Poisson summation formula (3.3)*. The error* (3.6) *has the upper bound*

$$\frac{1}{\sqrt{L}}\, \delta(f, P) + \sqrt{L}\, \delta(\hat{f}, L)\,,$$

which can be further estimated under concrete decay conditions on f and $\hat{f}$ by Lemma 3.9 and Lemma 3.15. For the discretized version of (3.6) *we obtain*

$$\frac{1}{\sqrt{L}} \max_{\ell \in [LP]} \left| f\left(\frac{\ell}{L}\right) - \frac{1}{P} \sum_{n \in [LP]} \hat{f}\Big(\frac{n}{P}\Big)\, \mathrm{e}^{2\pi \mathrm{i}\, n\ell/(LP)} \right| \le \frac{1}{\sqrt{L}}\, \delta(f, P) + \sqrt{L}\, \delta(\hat{f}, L)\,.$$

Remark 3.7. *The reconstruction in Remark 3.6 presupposes the exact Fourier samples $\hat{f}(n/P)$, $n \in [LP]$. In practice, however, only the computed trigonometric sampling polynomial $s_{P,L}$, see* (1.2)*, is available. We therefore sample $s_{P,L}$ on the finer equispaced grid $\big\{j/M : j \in [MP]\big\}$ of the frequency interval $[-P/2,\, P/2)$, where $M \in 2\mathbb{N}$ with $M \ge 2L$ denotes a frequency oversampling factor, and form the fully computable approximation*

$$f_{M,P,L}(x) := \frac{1}{M} \sum_{j \in [MP]} s_{P,L}\left(\frac{j}{M}\right) \mathrm{e}^{2\pi \mathrm{i}\, jx/M}\,, \qquad x \in [-L/2,\, L/2)\,. \tag{3.7}$$

This is the M-point rectangle-rule discretization of the truncated inverse Fourier integral $\int_{-P/2}^{P/2} s_{P,L}(v)\, \mathrm{e}^{2\pi \mathrm{i}\, vx}\, \mathrm{d}v$; on the grid $x = \ell/P$, $\ell \in [LP]$, it can be evaluated by a single inverse FFT *of length MP.*

Introducing the truncated cardinal series

$$g_{P,L}(x) := \int_{-P/2}^{P/2} s_{P,L}(v)\, \mathrm{e}^{2\pi \mathrm{i}\, vx}\, \mathrm{d}v = \sum_{n\in[LP]} f\Big(\frac{n}{P}\Big)\, \mathrm{sinc}\big(Px-n\big)\,, \qquad \mathrm{sinc}(t) := \frac{\sin(\pi t)}{\pi t}\,, \tag{3.8}$$

the approximation error splits into three contributions,

$$f(x) - f_{M,P,L}(x) = \underbrace{\int_{|v|>P/2} \hat{f}(v)\, \mathrm{e}^{2\pi \mathrm{i}\, vx}\, \mathrm{d}v}_{\textit{band truncation}} + \underbrace{\int_{-P/2}^{P/2} \big(\hat{f} - s_{P,L}\big)(v)\, \mathrm{e}^{2\pi \mathrm{i}\, vx}\, \mathrm{d}v}_{\textit{sampling polynomial}} + \underbrace{\big(g_{P,L}(x) - f_{M,P,L}(x)\big)}_{\textit{frequency discretization}}\,.$$

The first term is bounded by the L^1-tail $\eta(\hat{f},P) := \int_{|v|>P/2} |\hat{f}(v)|\, \mathrm{d}v$, the second by $P \max_{|v|\le P/2} |\hat{f}(v) - s_{P,L}(v)| = P\sqrt{L}\, M_{P,L}(f)$, see (1.5). For the third term, a direct evaluation of the geometric sum in (3.7) gives the closed form

$$f_{M,P,L}(x) = \frac{1}{MP} \sum_{n\in[LP]} f(n/P)\, \mathrm{e}^{\mathrm{i}\pi\alpha_n/M}\, \frac{\sin(\pi P\alpha_n)}{\sin(\pi\alpha_n/M)}$$

with $\alpha_n := x - n/P$, hence

$$g_{P,L}(x) - f_{M,P,L}(x) = \frac{1}{P} \sum_{n\in[LP]} f\Big(\frac{n}{P}\Big) \sin(\pi P\alpha_n) \left[\frac{1}{\pi\alpha_n} - \frac{\mathrm{e}^{\mathrm{i}\pi\alpha_n/M}}{M\, \sin(\pi\alpha_n/M)}\right].$$

Since $|\sin(\pi P\alpha_n)| \le 1$ and, by the elementary inequality $1 - \beta\cot\beta \le \beta^2$ for $|\beta| \le \pi/2$, the bracket is bounded in modulus by $M^{-1}\sqrt{1+\pi^2/4}$ whenever $|\alpha_n| \le M/2$ (which holds for $|x| \le L/2$ as $M \ge 2L$), we obtain with Lemma 3.1 (for $R = 1/P$ and $|x| \le L/2$)

$$\big|g_{P,L}(x) - f_{M,P,L}(x)\big| \le \frac{\sqrt{1+\pi^2/4}}{MP} \sum_{n\in[LP]} \Big|f\Big(\frac{n}{P}\Big)\Big| \le \frac{(P+1)\sqrt{1+\pi^2/4}}{MP}\, \|f\|_{W(C(\mathbb{R}),\ell^1(\mathbb{Z}))}\,.$$

Combining the three bounds with Theorem 3.5 and $(P+1)/P \le 2$ yields the uniform error estimate

$$\max_{|x|\le L/2} \big|f(x) - f_{M,P,L}(x)\big| \le \eta(\hat{f},P) + P\,\big(\delta(\hat{f},P) + L\,\delta(f,L)\big) + \frac{2\sqrt{1+\pi^2/4}}{M}\, \|f\|_{W(C(\mathbb{R}),\ell^1(\mathbb{Z}))}\,. \tag{3.9}$$

The three terms reflect, respectively, the truncation of the inverse transform to the band $[-P/2, P/2]$, the approximation of $\hat{f}$ by $s_{P,L}$ on that band, and the rectangle-rule discretization in the frequency variable.

If $\hat{f}$ has polynomial decay $\sup_v |\hat{f}(v)|\,(1+|v|)^b \le c < \infty$ with $b > 1$, then $\eta(\hat{f},P) \le \frac{2c}{b-1}\,(1+P/2)^{1-b}$, and with Lemma 3.9 the estimate (3.9) becomes

$$\max_{|x|\le L/2} \big|f(x) - f_{M,P,L}(x)\big| \;\le\; \frac{2c}{b-1}\left(1+\frac{P}{2}\right)^{1-b} + 2c\,(2^b-1)\,\zeta(b)\,P^{1-b} + PL\,\delta(f,L)$$

$$+ \quad \frac{2\sqrt{1+\pi^2/4}}{M}\,\|f\|_{W(C(\mathbb{R}),\ell^1(\mathbb{Z}))}\,. \tag{3.10}$$

For compactly supported f, where $\delta(f,L)=0$ for sufficiently large L, the spatial error therefore decays as $\mathcal{O}(P^{1-b})+\mathcal{O}(M^{-1})$, and balancing the two contributions suggests the choice $M \gtrsim P^{\,b-1}$. We remark that the leading M^{-1}-coefficient is in fact governed by $|s_{P,L}(P/2)| \approx |\hat{f}(P/2)|$, which is already small at the band edge, so that in practice the frequency discretization is markedly less critical than the truncation with respect to P.

Remark 3.8. *Roughly speaking, smoothness of f implies polynomial decay of $\hat{f}$, and smoothness of $\hat{f}$ implies polynomial decay of f. If each derivative $f^{(\ell)}$, $\ell = 0,\dots,b$, belongs to $L^1(\mathbb{R})$, then the Fourier transform of $f^{(\ell)}$ equals $(2\pi v\,\mathrm{i})^\ell\,\hat{f}(v)$ and is bounded on $\mathbb{R}$, so that*

$$\sup_{v\in\mathbb{R}} |\hat{f}(v)|\,(1+|v|)^b \le c < \infty\,.$$

Conversely, if each derivative $\hat{f}^{(\ell)}$, $\ell = 0,\dots,b$, belongs to $L^1(\mathbb{R})$, then the inverse Fourier transform of $\hat{f}^{(\ell)}$ equals $(-2\pi\mathrm{i}\,x)^\ell\,f(x)$ and is bounded on $\mathbb{R}$, so that

$$\sup_{x\in\mathbb{R}} |f(x)|\,(1+|x|)^b \le c < \infty\,.$$

Now we estimate the decay rate (3.2) of a function $f \in C(\mathbb{R})$ with polynomial decay.

Lemma 3.9. *Let $L \in 2\mathbb{N}$ be given. Assume that $f \in C(\mathbb{R})$ has polynomial decay*

$$\sup_{x\in\mathbb{R}} |f(x)|\,(1+|x|)^a \le c < \infty\,, \quad a > 1\,.$$

Then the decay rate of f with respect step size L can be estimated by

$$\delta(f,L) \le 2c\,(2^a-1)\,\zeta(a)\,L^{-a}\,, \tag{3.11}$$

where $\zeta(a)$ denotes the Riemann zeta function

$$\zeta(a) := \sum_{n=0}^{\infty}(n+1)^{-a} < 1 + \frac{1}{a-1}\,, \quad a > 1\,.$$

Further f belongs to $W(C(\mathbb{R}),\ell^1(\mathbb{Z}))$ with the norm

$$\|f\|_{W(C(\mathbb{R}),\ell^1(\mathbb{Z}))} \le 2c\,\zeta(a) < \infty\,.$$

Proof. By the polynomial decay of f, for all $k \in \mathbb{Z}\setminus\{0\}$ and $|x| \le L/2$ it holds that

$$\big|f(x+kL)\big| \le c\,\big(1+|x+kL|\big)^{-a} \le c\,\big(1+\big(|k|-\tfrac{1}{2}\big)L\big)^{-a}\,.$$

Hence it follows that

$$\delta(f,L) \;=\; \max_{|x|\le L/2} \sum_{k\in\mathbb{Z}\setminus\{0\}} \big|f(x+kL)\big|$$

$$\begin{aligned} &\leq \; 2c \sum_{k=1}^{\infty} \big(1 + \big(k - \tfrac{1}{2}\big) L\big)^{-a} = 2c\, L^{-a} \sum_{k=1}^{\infty} \big(k - \tfrac{1}{2} + \tfrac{1}{L}\big)^{-a} \\ &< \; 2c\, L^{-a} \sum_{n=0}^{\infty} \big(n + \tfrac{1}{2}\big)^{-a} = 2c\, \zeta\big(a, \tfrac{1}{2}\big)\; L^{-a}\,, \end{aligned}$$

where $\zeta\big(a, \frac{1}{2}\big) := \sum_{n=0}^{\infty} \big(n + \frac{1}{2}\big)^{-a}$ denotes the *Hurwitz zeta function*. By $\zeta\big(a, \frac{1}{2}\big) = 2^a \sum_{n=0}^{\infty} (2n+1)^{-a}$ we obtain

$$\begin{aligned} \zeta(a) &= \sum_{n=0}^{\infty} (2n+1)^{-a} + \sum_{n=0}^{\infty} (2n+2)^{-a} = \sum_{n=0}^{\infty} (2n+1)^{-a} + 2^{-a} \sum_{n=0}^{\infty} (n+1)^{-a} \\ &= 2^{-a}\, \zeta\big(a, \tfrac{1}{2}\big) + 2^{-a}\, \zeta(a) \end{aligned}$$

such that $\zeta\big(a, \frac{1}{2}\big) = (2^a - 1)\, \zeta(a)$, which gives (3.11). For $a \in 2\mathbb{N}$, explicit values of $\zeta(a)$ are known, namely $\zeta(a) = \frac{|B_a|}{2\, a!}\, (2\pi)^a$ with the *Bernoulli number* B_a (see [1, pp. 266–267]). The integral test for convergence of series provides that for $a > 1$,

$$\zeta(a) = \sum_{n=0}^{\infty} (n+1)^{-a} \leq 1 + \int_0^{\infty} (x+1)^{-a}\, \mathrm{d}x = 1 + \frac{1}{a-1}\,.$$

Obviously, we have $f \in W(C(\mathbb{R}), \ell^1(\mathbb{Z}))$, since it holds by assumption that

$$\|f\|_{W(C(\mathbb{R}), \ell^1(\mathbb{Z}))} \leq c \sum_{n=0}^{\infty} (1+n)^{-a} + c \sum_{n=1}^{\infty} \big(1 + (n-1)\big)^{-a} = 2c\, \zeta(a) < \infty\,.$$

This completes the proof. ■

Using the corresponding decay rates of f and $\hat{f}$ which have both polynomial decays, we can estimate the scaled uniform maximum error $M_{P,L}(f)$:

Theorem 3.10. *Let L, $P \in 2\mathbb{N}$ be given. If both functions f, $\hat{f} \in C(\mathbb{R})$ have polynomial decays*

$$\begin{aligned} \sup_{x \in \mathbb{R}} |f(x)|\, (1 + |x|)^a &\leq c < \infty\,, \quad a > 1\,, \\ \sup_{v \in \mathbb{R}} |\hat{f}(v)|\, (1 + |v|)^b &\leq d < \infty\,, \quad b > 1\,, \end{aligned}$$

then it holds the error estimate

$$M^*_{P,L}(f) \leq M_{P,L}(f) \leq 2d\, (2^b - 1)\, \zeta(b)\, L^{-1/2}\, P^{-b} + 2c\, (2^a - 1)\, \zeta(a)\, L^{-a+1/2}\,. \tag{3.12}$$

Proof. Using Theorem 3.5, it follows that

$$M^*_{P,L}(f) \leq M_{P,L}(f) \leq \frac{1}{\sqrt{L}}\, \delta(\hat{f}, P) + \sqrt{L}\, \delta(f, L)\,.$$

Then Lemma 3.9 provides that

$$\begin{aligned}\delta(\hat{f}, P) &\leq 2d\,(2^b - 1)\,\zeta(b)\,P^{-b}\,,\\ \delta(f, L) &\leq 2c\,(2^a - 1)\,\zeta(a)\,L^{-a}\,.\end{aligned}$$

This completes the proof. ■

Remark 3.11. *We compare Theorem 3.10 with the corresponding result of [8, Theorem 2.1]. From [8, Theorem 2.1] it follows that*

$$M^*_{P,L}(f) \leq E^*_{P,L}(f) \leq C\,(L^{-\alpha} + P^{-\beta})$$

with arbitrary $\alpha \in \big(0,\, a - \frac{1}{2}\big)$, $\beta \in \big(0,\, b - \frac{1}{2}\big)$, *and some constant* $C > 0$. *Our estimate* (3.12) *is explicit and more practicable, since all constants are described directly by the assumptions of Theorem 3.10, and it does not lose an arbitrarily small* $\varepsilon > 0$ *in the exponents. Moreover, using Theorem 3.10, the scaled Euclidean approximation error can be bounded by*

$$E^*_{P,L}(f) \leq \sqrt{LP}\,M^*_{P,L}(f) \leq 2d\,(2^b - 1)\,\zeta(b)\,P^{-b+1/2} + 2c\,(2^a - 1)\,\zeta(a)\,L^{1-a}\,P^{1/2}\,.$$

The estimate (3.12) is not symmetric in the two parameters: the decay of $\hat{f}$ enters with the full exponent b, whereas the decay of f enters with the reduced exponent $a - \frac{1}{2}$. Since the corresponding bound of [8, Theorem 2.1] *is* symmetric, we explain in the following two remarks where this difference comes from. It turns out that it is caused neither by the proof technique nor by the normalization, but by a genuine structural difference between the two error contributions σ_1 and σ_2 in the proof of Theorem 3.5.

Remark 3.12. *Let* f, $\hat{f}$ *have polynomial decay with exponents* a, b *as in Theorem 3.10. Consider the two remainders*

$$\sigma_1(v) = \sum_{k \in \mathbb{Z}\setminus\{0\}} \hat{f}(v + kP)\,, \qquad \sigma_2(v) = \frac{1}{P} \sum_{n \in \mathbb{Z}\setminus[LP]} f\Big(\frac{n}{P}\Big)\,\mathrm{e}^{-2\pi\mathrm{i}\,nv/P}$$

separately, and compare their maximum norm on $[-P/2,\, P/2]$ *with their quadratic mean* $\big(\frac{1}{P}\int_{-P/2}^{P/2} |\sigma_j(v)|^2\,\mathrm{d}v\big)^{1/2}$.

The aliasing *remainder* σ_1 *is a periodization of* $\hat{f}$. *It is non-oscillatory, and both its maximum and its quadratic mean are of the exact order* P^{-b}; *the quotient of the two is bounded above and below by absolute constants.*

The truncation *remainder* σ_2 *behaves completely differently. By the orthogonality of the exponentials* $\mathrm{e}^{-2\pi\mathrm{i}\,nv/P}$ *on* $[-P/2,\, P/2]$ *we have exactly*

$$\frac{1}{P}\int_{-P/2}^{P/2} |\sigma_2(v)|^2\,\mathrm{d}v = \frac{1}{P^2} \sum_{n \in \mathbb{Z}\setminus[LP]} \Big|f\Big(\frac{n}{P}\Big)\Big|^2 = \Theta\big(P^{-1}\,L^{1-2a}\big)\,,$$

so that the quadratic mean of σ_2 is of the order $P^{-1/2}\,L^{1/2-a}$, whereas for nonnegative f at $v=0$ all summands add up constructively and give

$$\max_{|v|\le P/2}|\sigma_2(v)| \;\ge\; |\sigma_2(0)| = \frac{1}{P}\sum_{n\in\mathbb{Z}\setminus[LP]} f\Big(\frac{n}{P}\Big) = \Theta\big(L^{1-a}\big)\,.$$

Here the two-sided order estimates presuppose a matching two-sided polynomial decay $c_0\,(1+|x|)^{-a} \le |f(x)| \le c\,(1+|x|)^{-a}$; the lower estimate for $|\sigma_2(0)|$ is exactly the one established in Theorem 3.20. Hence the maximum of σ_2 exceeds its quadratic mean by the factor $\sqrt{LP}$, while for σ_1 the two agree up to constants.

This is the source of the asymmetry. Passing from an averaged error to a uniform error costs nothing in the aliasing part but costs the full factor $\sqrt{LP}$ in the truncation part, and no symmetric bound for the uniform error can therefore exist. We add that after the normalization by $L^{-1/2}$ both error measures predict the same *rate in the truncation parameter, namely $L^{1/2-a}$; the difference between* (3.12) *and [8, Theorem 2.1] is confined to the aliasing parameter, where our bound is better by the factor $\sqrt{LP}$. This is confirmed numerically in Example 4.5 and Figure 4.4b.*

Remark 3.13. *The two error measures $M^*_{P,L}(f)$ and $E^*_{P,L}(f)$ are* not *equivalent. Indeed, for any f we have the elementary two-sided estimate*

$$1 \;\le\; \frac{E^*_{P,L}(f)}{M^*_{P,L}(f)} \;\le\; \sqrt{LP}\,, \tag{3.13}$$

since a maximum of LP numbers is at most their Euclidean norm and at least $(LP)^{-1/2}$ times that norm. Both bounds in (3.13) *are essentially attained:*

- *If the error is* truncation dominated, *i.e. if $\delta(\hat f, P) \ll L\,\delta(f,L)$, then by Remark 3.12 the quotient stays bounded. For the bandlimited function g of Example 4.5 one finds numerically $E^*_{P,L}(g)/M^*_{P,L}(g) \to 1.244$ as $L\to\infty$, independently of P.*
- *If the error is* aliasing dominated, *i.e. if $L\,\delta(f,L) \ll \delta(\hat f, P)$, the quotient grows like $\sqrt{LP}$. For the compactly supported B-spline M_2 with $L=2$ one measures $E^*_{P,L}/M^*_{P,L} = 22.18$ at $P=1024$, while $\sqrt{LP}=45.25$; see Figure 4.4b.*

Consequently, an estimate for $E^*_{P,L}(f)$ may overestimate $M^*_{P,L}(f)$ by a factor which grows without bound, and Theorem 3.10 cannot be recovered from [8, Theorem 2.1]. We stress in addition that $M_{P,L}(f)$, which controls the error at every *v with $|v|\le P/2$, is not comparable to $E^*_{P,L}(f)$ at all, since the latter contains no information about the values of $\hat f - s_{P,L}$ off the grid $\{k/L : k\in[LP]\}$.*

As known, a nontrivial function cannot be bandlimited and space-limited (see [23, pp. 103–104]). If f is space-limited or bandlimited, then we obtain simpler error estimates:

Corollary 3.14. *Let L, $P \in 2\mathbb{N}$ be given. If f, $\hat{f} \in C(\mathbb{R})$ satisfy*

$$\begin{aligned} \sup_{x\in\mathbb{R}} |f(x)|\,(1+|x|)^a &\leq c<\infty\,, \quad a>1\,, \\ \operatorname{supp}\hat{f} &\subseteq \left[-\tfrac{M}{2},\,\tfrac{M}{2}\right], \quad 0<M\leq P\,, \end{aligned}$$

then it holds the error estimate

$$M^*_{P,L}(f) \leq M_{P,L}(f) \leq 2c\,(2^a-1)\,\zeta(a)\,L^{1/2-a}\,.$$

If f, $\hat{f} \in C(\mathbb{R})$ satisfy

$$\begin{aligned} \operatorname{supp} f &\subseteq \left[-\tfrac{M}{2},\,\tfrac{M}{2}\right], \quad 0<M\leq L\,, \\ \sup_{v\in\mathbb{R}} |\hat{f}(v)|\,(1+|v|)^b &\leq d<\infty\,, \quad b>1\,, \end{aligned}$$

then it holds the error estimate

$$M^*_{P,L}(f) \leq M_{P,L}(f) \leq 2d\,(2^b-1)\,\zeta(b)\,L^{-1/2}\,P^{-b}\,.$$

Proof. This result follows immediately from Theorem 3.10. If $\operatorname{supp}\hat{f} \subseteq \left[-\frac{M}{2},\,\frac{M}{2}\right]$ and $M \leq P$, then $\hat{f}(v+kP)=0$ for all $k \in \mathbb{Z}\setminus\{0\}$ and $|v| \leq P/2$, so that $\delta(\hat{f},P)=0$. If $\operatorname{supp} f \subseteq \left[-\frac{M}{2},\,\frac{M}{2}\right]$ and $M \leq L$, then all samples $f\left(\frac{n}{P}\right)$ vanish for $n \in \mathbb{Z}\setminus[LP]$, so that $\delta(f,L)=0$. ■

Now we estimate the decay rate (3.2) of a function with exponential decay.

Lemma 3.15. *Let $L \in 2\mathbb{N}$ be given. Let $f \in C(\mathbb{R})$ be a function with exponential decay*

$$\sup_{x\in\mathbb{R}} |f(x)|\,\mathrm{e}^{r\,|x|^\alpha} \leq c<\infty\,, \quad r,\,\alpha>0\,.$$

Assume that in the case $0<\alpha<1$ it holds $r\,(L/2)^\alpha > \frac{1}{\alpha}-1$.
Then the decay rate of f with respect to step size L can be estimated by

$$\delta(f,L) \leq 2c\,\gamma(r,\alpha,L)\,\mathrm{e}^{-r\,(L/2)^\alpha} \tag{3.14}$$

with

$$\gamma(r,\alpha,L) := \begin{cases} 1+\frac{r^{1/\alpha}}{L\,(\alpha r(L/2)^\alpha-1+\alpha)} & 0<\alpha<1\,, \\ 1+\frac{1}{rL} & \alpha=1\,, \\ 1+\frac{2\,(r(L/2)^\alpha+b_\alpha)^{1/\alpha}-r^{1/\alpha}L}{4b_\alpha} & \alpha>1\,. \end{cases}$$

For $\alpha>1$, it holds $b_\alpha := \Gamma\left(\frac{1}{\alpha}+1\right)^{\alpha/(1-\alpha)}$. Further f belongs to $W(C(\mathbb{R}),\ell^1(\mathbb{Z}))$ and has the norm

$$\|f\|_{W(C(\mathbb{R}),\ell^1(\mathbb{Z}))} \leq 2c+\tfrac{2c}{\alpha}\,r^{-1/\alpha}\,\Gamma\left(\tfrac{1}{\alpha}\right)<\infty\,.$$

Proof. By the exponential decay of f, for all $k \in \mathbb{Z} \setminus \{0\}$ and $|x| \le L/2$ it holds that

$$\big|f(x+kL)\big| \le c\,\mathrm{e}^{-r\,|x+kL|^\alpha} \le c\,\mathrm{e}^{-r\,(L/2)^\alpha\,(2|k|-1)^\alpha}\,.$$

Hence it follows that

$$\begin{aligned}\delta(f,L) &= \max_{|x|\le L/2} \sum_{k\in\mathbb{Z}\setminus\{0\}} \big|f(x+kL)\big| \le 2c \sum_{k=1}^{\infty} \mathrm{e}^{-r\,(L/2)^\alpha\,(2k-1)^\alpha} \\ &= 2c \sum_{n=0}^{\infty} \mathrm{e}^{-r\,(L/2)^\alpha\,(2n+1)^\alpha}\,.\end{aligned}$$

Setting $u := r\,(L/2)^\alpha$ for shortness, the integral test for convergence of series yields

$$\sum_{n=0}^{\infty} \mathrm{e}^{-u\,(2n+1)^\alpha} \le \mathrm{e}^{-u} + \int_0^{\infty} \mathrm{e}^{-u\,(2x+1)^\alpha}\,\mathrm{d}x = \mathrm{e}^{-u} + \frac{1}{2\alpha}\,u^{-1/\alpha}\,\Gamma\big(\tfrac{1}{\alpha},u\big)\,,$$

where

$$\Gamma\big(\frac{1}{\alpha},u\big) := \int_u^{\infty} t^{1/\alpha-1}\,\mathrm{e}^{-t}\,\mathrm{d}t$$

denotes the *upper incomplete gamma function*. A simple check shows that

$$-\frac{1}{\alpha}\,u^{-1/\alpha}\,\Gamma\big(\tfrac{1}{\alpha},t^\alpha\,u\big)$$

is a primitive of $\mathrm{e}^{-u\,t^\alpha}$ and therefore

$$\int_1^{\infty} \mathrm{e}^{-u\,t^\alpha}\,\mathrm{d}t = \frac{1}{\alpha}\,u^{-1/\alpha}\,\Gamma\big(\tfrac{1}{\alpha},u\big)\,.$$

By [22, Theorem 1.1 and Proposition 2.7], an upper bound of the upper incomplete gamma function $\Gamma\big(\frac{1}{\alpha},u\big)$ is given by

$$\Gamma\big(\tfrac{1}{\alpha},u\big) \le \begin{cases} \frac{u^{1/\alpha}}{u+1-1/\alpha}\,\mathrm{e}^{-u} & 0<\alpha<1\,, \\ \big(1+\frac{1}{2u}\big)\,\mathrm{e}^{-u} & \alpha=1\,, \\ \frac{\alpha\,(u+b_\alpha)^{1/\alpha}-u^{1/\alpha}}{b_\alpha}\,\mathrm{e}^{-u} & \alpha>1\,. \end{cases}$$

This implies the estimate (3.14). Obviously, we have $f \in W(C(\mathbb{R}),\ell^1(\mathbb{Z}))$, since it holds by assumption and [11, Formula 3.478] that

$$\begin{aligned}\|f\|_{W(C(\mathbb{R}),\ell^1(\mathbb{Z}))} &\le c\sum_{n=0}^{\infty}\mathrm{e}^{-r\,n^\alpha} + c\sum_{n=1}^{\infty}\mathrm{e}^{-r\,(n-1)^\alpha} = 2c\sum_{n=0}^{\infty}\mathrm{e}^{-r\,n^\alpha} \\ &\le 2c + 2c\int_0^{\infty}\mathrm{e}^{-r\,t^\alpha}\,\mathrm{d}t = 2c + \tfrac{2c}{\alpha}\,r^{-1/\alpha}\,\Gamma\big(\tfrac{1}{\alpha}\big) < \infty\,.\end{aligned}$$

This completes the proof. ■

Using the decay rates of f and $\hat{f}$ which have both exponential decays, we can estimate the scaled uniform maximum error $M_{P,L}(f)$:

Theorem 3.16. *Let L, $P \in 2\mathbb{N}$ be given. Let f, $\hat{f} \in C(\mathbb{R})$ be functions with exponential decay*

$$\begin{aligned} \sup_{x\in\mathbb{R}} |f(x)|\, \mathrm{e}^{r\,|x|^\alpha} &\leq c < \infty\,, \quad r,\, \alpha > 0\,, \\ \sup_{v\in\mathbb{R}} |\hat{f}(v)|\, \mathrm{e}^{s\,|v|^\beta} &\leq d < \infty\,, \quad s,\, \beta > 0\,. \end{aligned}$$

Assume that $r\,(L/2)^\alpha > \frac{1}{\alpha} - 1$ in the case $0 < \alpha < 1$ and that $s\,(P/2)^\beta > \frac{1}{\beta} - 1$ in the case $0 < \beta < 1$.
Then it holds the error estimate

$$M_{P,L}(f) \leq 2d\,\gamma(s,\beta,P)\,L^{-1/2}\,\mathrm{e}^{-s\,(P/2)^\beta} + 2c\,\gamma(r,\alpha,L)\,L^{1/2}\,\mathrm{e}^{-r\,(L/2)^\alpha}\,, \tag{3.15}$$

where the constants $\gamma(s,\beta,P)$ and $\gamma(r,\alpha,L)$ are defined in Lemma 3.15.

Proof. Using Theorem 3.5, it follows that

$$M_{P,L}(f) \leq \frac{1}{\sqrt{L}}\,\delta(\hat{f},P) + \sqrt{L}\,\delta(f,L)\,.$$

Then Lemma 3.15 provides that

$$\begin{aligned} \delta(\hat{f},P) &\leq 2d\,\gamma(s,\beta,P)\,\mathrm{e}^{-s\,(P/2)^\beta}\,, \\ \delta(f,L) &\leq 2c\,\gamma(r,\alpha,L)\,\mathrm{e}^{-r\,(L/2)^\alpha}\,. \end{aligned}$$

This completes the proof. ■

Remark 3.17. *We compare Theorem 3.16 with the corresponding result in [8, Theorem 2.3]. Then from [8, Theorem 2.3] it follows immediately that*

$$M^*_{P,L}(f) \leq E^*_{P,L}(f) \leq C\left(\mathrm{e}^{-r'(L/2)^\alpha} + \mathrm{e}^{-s'(P/2)^\beta}\right)$$

with arbitrary $r' \in (0,\,r)$, $s' \in (0,\,s)$, and certain constant $C > 0$. Note that in [8, Theorem 2.3] it is considered only the case $0 < \alpha,\, \beta \leq 1$. Thus we see that our estimate (3.15) *is more general, explicit, and more practicable, since all constants in* (3.15) *are known from the decay conditions of Theorem 3.16.*

Using the decay rates of f and $\hat{f}$ which have mixed decays, we can estimate the scaled uniform maximum error $M_{P,L}(f)$:

Theorem 3.18. *Let L, $P \in 2\mathbb{N}$ be given. Let f, $\hat{f} \in C(\mathbb{R})$ be functions with mixed decay*

$$\begin{aligned} \sup_{x\in\mathbb{R}} |f(x)|\,(1+|x|)^a &\leq c < \infty\,, \quad a > 1\,, \\ \sup_{v\in\mathbb{R}} |\hat{f}(v)|\, \mathrm{e}^{s\,|v|^\beta} &\leq d < \infty\,, \quad s,\, \beta > 0\,. \end{aligned}$$

Assume that $s\,(P/2)^\beta > \frac{1}{\beta} - 1$ *in the case* $0 < \beta < 1$. *Then it holds the error estimate*

$$M_{P,L}(f) \le 2d\,\gamma(s,\beta,P)\,L^{-1/2}\,\mathrm{e}^{-s\,(P/2)^\beta} + 2c\,(2^a-1)\,\zeta(a)\,L^{-a+1/2}\,.$$

Alternatively, let $f,\ \hat{f} \in C(\mathbb{R})$ *be functions with mixed decay*

$$\begin{aligned} \sup_{x\in\mathbb{R}} |f(x)|\,\mathrm{e}^{r\,|x|^\alpha} &\le c < \infty\,, \quad r,\,\alpha > 0\,, \\ \sup_{v\in\mathbb{R}} |\hat{f}(v)|\,(1+|v|)^b &\le d < \infty\,, \quad b > 1\,. \end{aligned}$$

Assume that $r\,(L/2)^\alpha > \frac{1}{\alpha} - 1$ *in the case* $0 < \alpha < 1$. *Then it holds the error estimate*

$$M_{P,L}(f) \le 2d\,(2^b-1)\,\zeta(b)\,L^{-1/2}\,P^{-b} + 2c\,\gamma(r,\alpha,L)\,L^{1/2}\,\mathrm{e}^{-r\,(L/2)^\alpha}\,. \tag{3.16}$$

Proof. In both cases, Theorem 3.5 yields

$$M_{P,L}(f) \le \frac{1}{\sqrt{L}}\,\delta(\hat{f},P) + \sqrt{L}\,\delta(f,L)\,.$$

Then the assertion follows immediately from Lemma 3.9 and Lemma 3.15. ■

In practice, $L,\ P \in 2\mathbb{N}$ are sufficiently large, so that the exponential error terms in the estimates of Theorem 3.18 are negligible. Thus $M_{P,L}(f)$ is dominated by the corresponding polynomial error term.

Remark 3.19. *We compare the second case of Theorem 3.18 with the corresponding result in [8, Theorem 2.4]. Then from [8, Theorem 2.4 and (4.21)] it follows immediately that*

$$M^*_{P,L}(f) \le E^*_{P,L}(f) \le C\left(\mathrm{e}^{-r'(L/2)^\alpha} + P^{-\beta}\right)$$

with arbitrary $r' \in (0,\,r)$, $\beta \in \left(0,\,b-\frac{1}{2}\right)$, *and certain constant* $C > 0$. *Note that in [8, Theorem 2.4] it is considered only the case* $0 < \alpha \le 1$. *Thus we see that our estimate* (3.16) *is more general, explicit, and more practicable, since all constants in* (3.16) *are known from the decay conditions of Theorem 3.18.*

3.4 A lower bound for the uniform approximation error

All estimates obtained so far are upper bounds. We now show that the rate in the truncation parameter L predicted by Theorem 3.10 is sharp. This is in particular relevant for Remark 3.12, where we claimed that the asymmetry of (3.12) is a genuine effect.

Theorem 3.20. *Let* $L,\ P \in 2\mathbb{N}$ *be given, and let* $f \in W(C(\mathbb{R}),\ell^1(\mathbb{Z}))$ *with* $\hat{f} \in W(C(\mathbb{R}),\ell^1(\mathbb{Z}))$. *Assume that* f *is nonnegative, that* f *is non-increasing on* $[x_0,\,\infty)$ *for some* $x_0 \ge 0$, *and that*

$$f(x) \;\ge\; c_0\,(1+x)^{-a}\,, \qquad x \ge x_0\,,$$

with constants $c_0 > 0$ and $a > 1$. Then for all $L \geq 2\,x_0$ it holds

$$M_{P,L}(f) \;\geq\; M^*_{P,L}(f) \;\geq\; \frac{1}{\sqrt{L}} \left(\frac{c_0}{a-1} \left(1 + \frac{L}{2} + \frac{1}{P} \right)^{1-a} - \delta(\hat{f}, P) \right). \tag{3.17}$$

The bound (3.17) *is informative in the truncation dominated regime $\delta(\hat{f}, P) < \frac{c_0}{a-1}(1 + \frac{L}{2} + \frac{1}{P})^{1-a}$. In particular, if $\hat{f}$ is bandlimited with* $\operatorname{supp} \hat{f} \subseteq [-\frac{M}{2}, \frac{M}{2}]$ *and $M \leq P$, then $\delta(\hat{f}, P) = 0$ and*

$$M_{P,L}(f) \;\geq\; \frac{c_0}{a-1} \left(1 + \frac{L}{2} + \frac{1}{P} \right)^{1-a} L^{-1/2} \;=\; \Omega\big(L^{-a+1/2}\big) \qquad (L \to \infty)\,,$$

uniformly in $P \geq M$. Together with the upper bound $\mathcal{O}(L^{-a+1/2})$ of Theorem 3.10 and Corollary 3.14, this yields the two-sided estimate $M_{P,L}(f) = \Theta\big(L^{-a+1/2}\big)$.

Proof. As in the proof of Theorem 3.5 we have $\hat{f}(v) - s_{P,L}(v) = \sigma_2(v) - \sigma_1(v)$ for all $v \in \mathbb{R}$. Evaluating at the grid point $v = 0$, which belongs to $\{k/L : k \in [LP]\}$, we obtain

$$\sqrt{L}\, M^*_{P,L}(f) \;\geq\; \big|\hat{f}(0) - s_{P,L}(0)\big| = \big|\sigma_2(0) - \sigma_1(0)\big| \;\geq\; |\sigma_2(0)| - |\sigma_1(0)|\,.$$

By the proof of Theorem 3.5 we have $|\sigma_1(0)| \leq \delta(\hat{f}, P)$. Since $f \geq 0$, the value

$$\sigma_2(0) = \frac{1}{P} \sum_{n \in \mathbb{Z} \setminus [LP]} f\Big(\frac{n}{P}\Big)$$

is nonnegative, so that $|\sigma_2(0)| = \sigma_2(0)$, and discarding the indices $n \leq -\frac{LP}{2}$ only decreases the sum,

$$\sigma_2(0) \;\geq\; \frac{1}{P} \sum_{n > LP/2} f\Big(\frac{n}{P}\Big) = \frac{1}{P} \sum_{n \geq LP/2+1} f\Big(\frac{n}{P}\Big)\,.$$

Since $L \geq 2x_0$, the function f is non-increasing on $[\frac{L}{2}, \infty)$, and the right-hand side is a lower Riemann sum with step size $\frac{1}{P}$ of the integral of f over $\big[\frac{L}{2} + \frac{1}{P}, \infty\big)$. Hence

$$\sigma_2(0) \;\geq\; \int_{L/2+1/P}^{\infty} f(x)\,\mathrm{d}x \;\geq\; c_0 \int_{L/2+1/P}^{\infty} (1+x)^{-a}\,\mathrm{d}x = \frac{c_0}{a-1} \left(1 + \frac{L}{2} + \frac{1}{P} \right)^{1-a}.$$

Together with $M^*_{P,L}(f) \leq M_{P,L}(f)$ this gives (3.17). ■

Remark 3.21. *Theorem 3.20 shows that the exponent $a - \frac{1}{2}$ of L in* (3.12) *is optimal, and that the maximum of $|\hat{f} - s_{P,L}|$ is, in the truncation dominated regime, attained near $v = 0$ and is of the order of the L^1-tail $\int_{|x|>L/2} |f(x)|\,\mathrm{d}x$ of f. The assumptions of Theorem 3.20 are satisfied, e.g., by the bandlimited function g of Example 4.5 and, more generally, by every nonnegative even function with a monotone tail of exact polynomial order. They are not satisfied by oscillating functions, for which cancellation in $\sigma_2(0)$ may occur; in that case the upper bound of Theorem 3.10 need not be attained.*

3.5 The resulting algorithm

We now summarize the method. The input consists of the function f, the decay data of f and $\hat{f}$, a target accuracy $\varepsilon > 0$ and the nodes at which $\hat{f}$ is to be evaluated. The output consists of approximate values of $\hat{f}$ together with a rigorous a priori error bound.

Algorithm 3.22 (Computation of the Fourier transform via NFFT)**.**

Input: *$f \in W(C(\mathbb{R}), \ell^1(\mathbb{Z}))$ with $\hat{f} \in W(C(\mathbb{R}), \ell^1(\mathbb{Z}))$, given as a routine which evaluates f; decay parameters of f and $\hat{f}$ as in Theorem 3.10, Theorem 3.16 or Theorem 3.18; target accuracy $\varepsilon > 0$; evaluation nodes $v_1, \dots, v_K \in \mathbb{R}$.*

1. Choice of the bandwidth P. *Choose $P \in 2\mathbb{N}$ with $P \geq 2 \max_j |v_j|$, so that all evaluation nodes lie in $[-P/2,\, P/2]$, and so large that the aliasing term satisfies $\delta(\hat{f}, P) \leq \frac{\varepsilon}{2}$. For polynomial decay of $\hat{f}$ this means $2d\,(2^b - 1)\,\zeta(b)\,P^{-b} \leq \frac{\varepsilon}{2}$ by Lemma 3.9; for exponential decay use Lemma 3.15.*

2. Choice of the truncation parameter L. *Choose $L \in 2\mathbb{N}$ so large that the truncation term satisfies $L\,\delta(f, L) \leq \frac{\varepsilon}{2}$, again by Lemma 3.9 or Lemma 3.15. By Theorem 3.5 the resulting sampling polynomial then satisfies $\max_{|v| \leq P/2} |\hat{f}(v) - s_{P,L}(v)| \leq \varepsilon$.*

3. Sampling. *Evaluate f at the LP equispaced nodes n/P, $n \in [LP]$, and form the coefficients $c_n := \frac{1}{P}\, f\big(\frac{n}{P}\big)$.*

4. Choice of the NFFT parameters. *Choose the oversampling factor $\sigma \geq 1$ (usually $\sigma = 2$) and the window cut-off parameter $m \in \mathbb{N}$ so that the* NFFT *error is below ε; by [24, 25] the* NFFT *error decays exponentially in m, and in practice $m \leq 8$ suffices, see Table 5.3.*

5. Evaluation. *Compute $s_{P,L}(v_j) = \sum_{n \in [LP]} c_n\, \mathrm{e}^{-2\pi \mathrm{i}\, n(v_j/P)}$, $j = 1, \dots, K$, by one* NFFT *of size LP with the nodes $x_j := v_j/P \in [-\frac{1}{2}, \frac{1}{2})$. If the v_j are the equispaced points k/L, $k \in [LP]$, replace the* NFFT *by a single* FFT *of length LP.*

Output: *approximate values $s_{P,L}(v_j) \approx \hat{f}(v_j)$, $j = 1, \dots, K$, with the guarantee $\max_j |\hat{f}(v_j) - s_{P,L}(v_j)| \leq \sqrt{L}\, M_{P,L}(f) \leq \varepsilon$ up to the* NFFT *error of step 4.*

Cost: *$\mathcal{O}(LP)$ evaluations of f in step 3 and $\mathcal{O}\big(\sigma LP \log(\sigma LP) + m\,K\big)$ arithmetic operations in step 5.*

Remark 3.23. *The total error of Algorithm 3.22 splits into the approximation error analysed in this paper and the error of the* NFFT *itself,*

$$\big|\hat{f}(v_j) - \tilde{s}_{P,L}(v_j)\big| \;\leq\; \underbrace{\max_{|v| \leq P/2} \big|\hat{f}(v) - s_{P,L}(v)\big|}_{\leq \sqrt{L}\, M_{P,L}(f),\ \text{Theorem 3.5}} \;+\; \underbrace{\big|s_{P,L}(v_j) - \tilde{s}_{P,L}(v_j)\big|}_{\text{NFFT error, see [24, 25]}},$$

where $\tilde{s}_{P,L}$ denotes the value actually computed by the NFFT*. It is essential here that the first term is bounded* uniformly *in v, because the nodes v_j are arbitrary; a bound on the grid $\{k/L\}$ only, as provided by [8], would not suffice. Since the* NFFT *error decays exponentially in the cut-off parameter m, the second term can always be made negligible against the first at a cost which is linear in m; see Table 5.3.*

4 Numerical examples

In the previous section, we derived explicit error estimates for the uniform approximation error $M_{P,L}(f)$ under polynomial, exponential, and mixed decay conditions on f and $\hat{f}$. We now illustrate these theoretical bounds by means of concrete examples. For each example, we specify the relevant decay parameters and state the resulting error estimate from Section 3 explicitly before comparing it numerically with the true approximation error $M_{P,L}(f)$.

Example 4.1. *Let M_2 be the centered linear B-spline given by*

$$M_2(x) := \begin{cases} 1 - |x| & x \in [-1,\, 1]\,, \\ 0 & x \in \mathbb{R} \setminus [-1,\, 1]\,. \end{cases}$$

Then $f = M_2$ has the Fourier transform

$$\hat{f}(v) = \int_{-1}^{1} (1 - |x|)\, \cos(2\pi v x)\, \mathrm{d}x = \big(\operatorname{sinc}(\pi v)\big)^2\,, \quad v \in \mathbb{R}\,.$$

Since $\operatorname{supp} f = [-1,\, 1]$*, the function $f \in C(\mathbb{R})$ is space-limited with $M = 2$, and $\hat{f} \in C(\mathbb{R})$ has polynomial decay with $b = 2$. If we estimate the even function $\hat{f}(v)\,(1 + |v|)^2$ separately on the intervals $[0,\, \frac{1}{2}]$ and $[\frac{1}{2},\, \infty)$, we see that $d = \frac{9}{4}$ is a possible choice. By Corollary 3.14, for any $L \geq 2$ it holds*

$$M_{P,L}(f) \leq 2d\,(2^2 - 1)\,\zeta(2)\,L^{-1/2}\,P^{-2} = \frac{\pi^2}{\sqrt{L}}\,d\,P^{-2}\,.$$

Hence the error decays like P^{-2} as $P \to \infty$, which is confirmed by the numerical results in Figure 4.1a (left). More generally, for the B-spline M_{2m} of even order $2m$, the Fourier transform $\widehat{M_{2m}}$ has polynomial decay with $b = 2m$, and Corollary 3.14 yields the estimate

$$M_{P,L}(f) \leq 2d\,(2^{2m} - 1)\,\zeta(2m)\,L^{-1/2}\,P^{-2m}\,.$$

This P^{-2m} decay is illustrated in Figure 4.1b (right, $m = 2$) and Figure 4.2a ($m = 3$).

Alternatively, consider the bandlimited function

$$g(x) := \frac{M}{2}\,\left(\operatorname{sinc}\left(\frac{M}{2}\,\pi x\right)\right)^2\,, \quad x \in \mathbb{R}\,,$$

whose Fourier transform is $\hat{g}(v) = M_2\big(\frac{2}{M}\,v\big)$ with $\operatorname{supp}\hat{g} \subseteq \big[-\frac{M}{2},\, \frac{M}{2}\big]$. Since g has polynomial decay with $a = 2$, Corollary 3.14 gives, for $P \geq M$,

$$M_{P,L}(g) \leq 2c\,(2^2 - 1)\,\zeta(2)\,L^{1/2-2} = \pi^2\,c\,L^{-3/2}\,.$$

Hence the error decays like $L^{-3/2}$ as $L \to \infty$, which is confirmed numerically in Example 4.5 and Figure 4.4a.

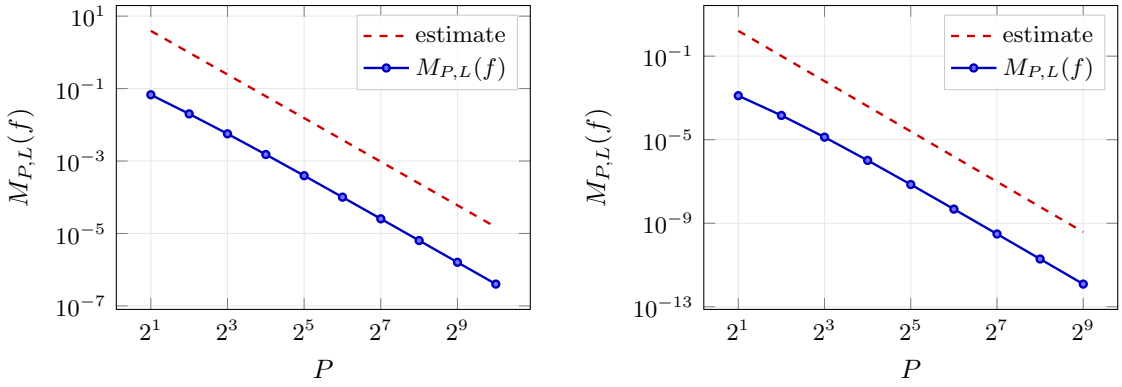

(a) B-Spline M_2, order 2 ($L = 2$)

(b) B-Spline M_4, order 4 ($L = 4$)

Figure 4.1: Estimate (3.12) (Corollary 3.14) and simulated error $M_{P,L}(f)$ for Example 4.1: the B-spline M_2 of order 2 with $L = 2$ (left, decay P^{-2}) and M_4 of order 4 with $L = 4$ (right, decay P^{-4}).

Example 4.2. *The Gaussian function*

$$f(x) = \mathrm{e}^{-\pi x^2}, \quad x \in \mathbb{R},$$

has exponential decay with $r = \pi$ and $\alpha = 2$, and its Fourier transform $\hat{f}(v) = \mathrm{e}^{-\pi v^2}$ has the same exponential decay with $s = \pi$ and $\beta = 2$. Provided $\pi\,(L/2)^2 \geq 1$ and $\pi\,(P/2)^2 \geq 1$, Theorem 3.16 yields

$$M_{P,L}(f) \leq \frac{1}{\sqrt{L}} \left(2 \left(1 + \frac{1}{8} \right) \mathrm{e}^{-\pi\,(P/2)^2} + 2 \left(1 + \frac{1}{8} \right) L\, \mathrm{e}^{-\pi\,(L/2)^2} \right) \tag{4.1}$$

$$= \frac{9}{4\sqrt{L}} \left(\mathrm{e}^{-\pi P^2/4} + L\, \mathrm{e}^{-\pi L^2/4} \right). \tag{4.2}$$

For fixed $L = P$ we obtain

$$M_{L,L}(f) \leq \frac{9(L+1)}{4\sqrt{L}}\, \mathrm{e}^{-\pi L^2/4}.$$

In Figure 4.2b we plot the error $M_{P,P}$ as well as the analytical estimate for $P = 1, \ldots 8$.

Example 4.3. *This example is taken from [8, Section 3.2], where it is used to illustrate the mixed-decay case for the scaled Euclidean error; we use it here in order to make the two sets of results directly comparable, and additionally in Section 5. Let*

$$f(x) := \mathrm{e}^{-2\pi\,|x-\delta|}, \quad x \in \mathbb{R},$$

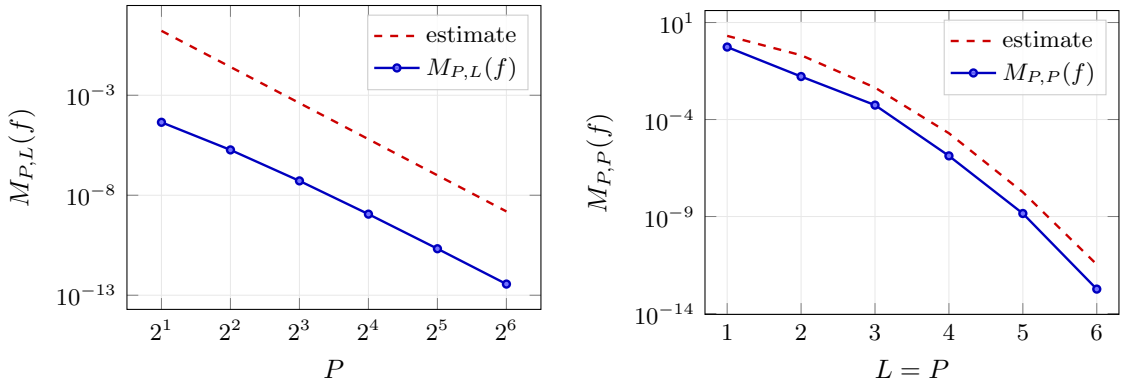

(a) B-Spline M_6, order 6 ($L = 6$)

(b) Gaussian $e^{-\pi x^2}$ ($L = P$)

Figure 4.2: Estimate and simulated error $M_{P,L}(f)$: the B-spline M_6 of order 6 with $L = 6$ for Example 4.1 (left, estimate (3.12), decay P^{-6}) and the Gaussian $\mathrm{e}^{-\pi x^2}$ with $L = P$ for Example 4.2 (right, estimate $\frac{9(L+1)}{4\sqrt{L}}\,\mathrm{e}^{-\pi L^2/4}$).

with shift parameter $\delta \in \mathbb{R}$. Its Fourier transform is

$$\hat{f}(v) = \frac{\mathrm{e}^{-2\pi \mathrm{i}\,\delta v}}{\pi\,(1+v^2)}\,, \quad v \in \mathbb{R}\,.$$

Hence f has exponential decay with $r = 2\pi$ and $\alpha = 1$, and $\hat{f}$ has polynomial decay with $b = 2$ and constant $d = 1/\pi$. This is the mixed-decay case of Theorem 3.18. Provided $2\pi\,(L/2) \geq 1$, i.e., $L \geq 1/\pi$, we obtain

$$M_{P,L}(f) \leq \frac{1}{\sqrt{L}}\left(\frac{2}{\pi}\,(2^2-1)\,\zeta(2)\,P^{-2} + 2\left(1+\frac{1}{2}\right)L\,\mathrm{e}^{-2\pi\,(L/2)}\right) = \frac{1}{\sqrt{L}}\left(\frac{2\pi}{P^2} + 3L\,\mathrm{e}^{-\pi L}\right).$$

For sufficiently large L, the exponential term is negligible, and the error is dominated by the polynomial term $\frac{2\pi}{\sqrt{L}\,P^2}$. A good parameter choice is $L = 8$ and $P = 2^t$, $t \geq 6$; for these values the exponential contribution is below machine precision and the estimate reduces to $M_{P,L}(f) \approx \frac{2\pi}{\sqrt{8}\,P^2}$, confirming the observed P^{-2} decay in Figure 4.3a.

Example 4.4. *For fixed parameter $\beta \in \mathbb{N}$ we consider the function*

$$f(x) := \begin{cases} (1-x^2)^{\beta-1/2} & x \in [-1,\,1]\,, \\ 0 & x \in \mathbb{R} \setminus \big[-1,\,1\big]\,. \end{cases}$$

Using [21, p. 8], we determine the corresponding Fourier transform

$$\begin{aligned} \hat{f}(v) &= \int_{-1}^{1} (1-x^2)^{\beta-1/2}\,\mathrm{e}^{-2\pi\mathrm{i}\,vx}\,\mathrm{d}x = 2\int_{0}^{1} (1-x^2)^{\beta-1/2}\,\cos(2\pi\,vx)\,\mathrm{d}x \\ &= \frac{\pi\,(2\beta)!}{4^\beta\,\beta!}\begin{cases} (\pi v)^{-\beta}\,J_\beta(2\pi v) & v \in \mathbb{R}\setminus\{0\}\,, \\ \frac{1}{\beta!} & v = 0\,. \end{cases} \end{aligned} \tag{4.3}$$

and obtain the estimate [24, Section 5.3]

$$|\hat{f}(v)| \le \frac{3\,(2\beta)!}{2^{3/2}\,4^{\beta}\,\beta!\,\pi^{\beta-1/2}}\,|v|^{-\beta-1/2}\,. \tag{4.4}$$

For $\beta = 2$ we observe by Corollary 3.14 with $M = 1$ and $b = 2$ the decay $P^{-2.5}$, see Figure 4.3b.

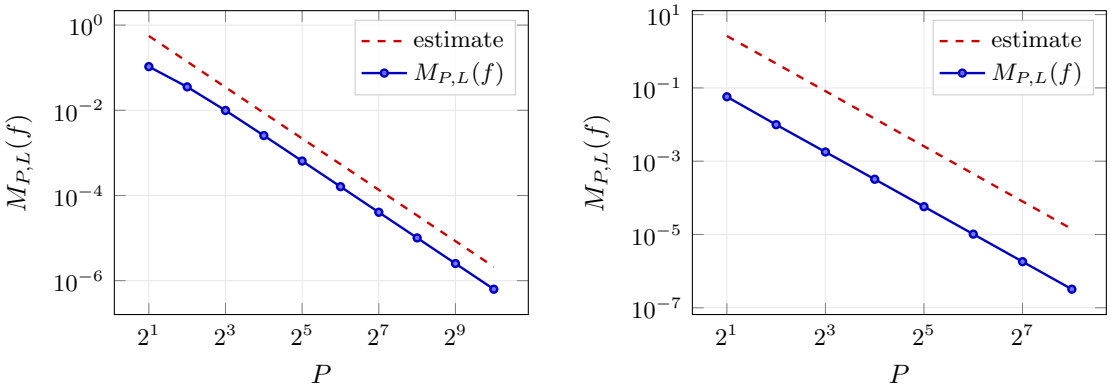

(a) mixed decay: $f(x) = \mathrm{e}^{-2\pi|x|}$ $(L = 8)$

(b) algebraic decay: $f(x) = (1 - x^2)^{3/2}$ for $x \in [-1, 1]$ $(L = 2)$

Figure 4.3: Estimate and simulated error $M_{P,L}(f)$ for Example 4.3 with $L = 8$ (left, decay P^{-2}) and Example 4.4 with $L = 2$ (right, decay $P^{-2.5}$).

Example 4.5. *So far all experiments were carried out for a fixed truncation parameter L and increasing bandwidth P, i.e. they probe the aliasing term $L^{-1/2}\,\delta(\hat{f}, P)$ of (3.5). We now isolate the* truncation *term $L^{1/2}\,\delta(f, L)$ and keep P fixed while L increases. To this end we use the bandlimited function of Example 4.1,*

$$g(x) = \frac{M}{2}\left(\operatorname{sinc}\left(\tfrac{M}{2}\,x\right)\right)^2, \qquad \hat{g}(v) = M_2\left(\frac{2v}{M}\right), \qquad M = 2\,,$$

for which $\operatorname{supp}\hat{g} \subseteq [-1,\,1]$, hence $\delta(\hat{g}, P) = 0$ for all $P \ge 2$, and g has polynomial decay with $a = 2$ and $c = \sup_x |g(x)|(1 + |x|)^2 = 1.267505$. By Corollary 3.14 we obtain the estimate

$$M_{P,L}(g) \;\le\; 2c\,(2^2 - 1)\,\zeta(2)\,L^{-3/2} = \pi^2 c\,L^{-3/2}\,,$$

and by Theorem 3.20 the matching lower bound of the same order $L^{-3/2}$.

Figure 4.4a shows the measured errors for $L = 2^1, \ldots, 2^9$ and $P = 8$. The observed convergence order, computed from consecutive values, is -1.457, -1.487, -1.497, -1.499, -1.500, -1.500, -1.500, -1.500, i.e. it converges to the predicted exponent $-\frac{3}{2} = \frac{1}{2} - a$. Repeating the experiment with $P = 32$ reproduces the same values to five significant digits, which confirms that the truncation term of (3.5) is indeed independent of P.

The same figure shows the scaled Euclidean error $E^*_{P,L}(g)$ of [8]. In this truncation dominated regime both errors have the same order, and the quotient $E^*_{P,L}(g)/M^*_{P,L}(g)$ increases monotonically from 1.216 *at* $L = 2$ *to the limit* 1.244*, in agreement with Remark 3.12. Hence, for this class of functions, our uniform estimate loses nothing compared with the Euclidean estimate, although it controls the error at every v and not only at the LP grid points.*

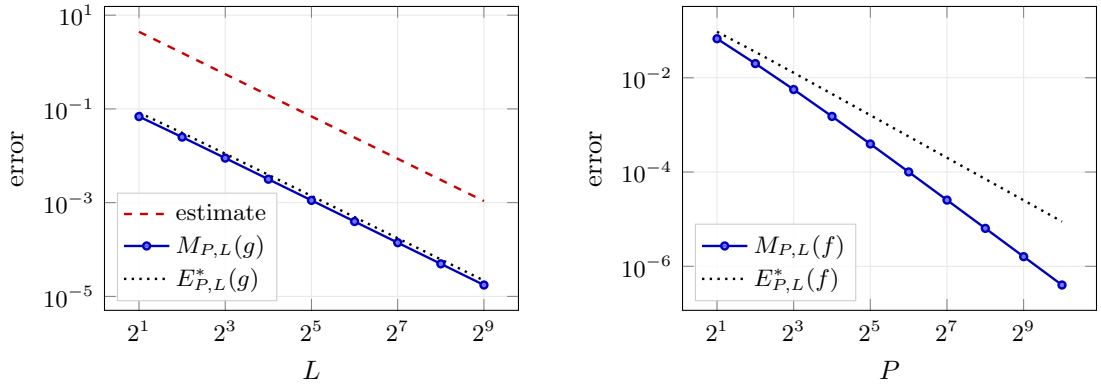

(a) fixed $P = 8$, increasing L (decay $L^{-3/2}$)

(b) $f = M_2$, $L = 2$: P^{-2} versus $P^{-3/2}$

Figure 4.4: Left: truncation dominated regime of Example 4.5; both error measures decay like $L^{-3/2}$ and their quotient tends to 1.244. Right: aliasing dominated regime (B-spline M_2, $L = 2$); the scaled maximum error decays like $P^{-b} = P^{-2}$, the scaled Euclidean error only like $P^{-b+1/2} = P^{-3/2}$, so that their quotient grows like $\sqrt{LP}$, cf. Remark 3.13.

5 Computational cost

The estimates of Section 3 answer the question how accurate the sampling polynomial $s_{P,L}$ is. We now address the complementary question how expensive it is to evaluate it, and compare the three possibilities listed in Algorithm 3.22:

- *direct evaluation* of (1.2) at K nodes, which requires $\mathcal{O}(LPK)$ arithmetic operations,
- the FFT, which delivers the LP values $s_{P,L}(k/L)$, $k \in [LP]$, on the equispaced grid in $\mathcal{O}(LP \log LP)$ operations,
- the NFFT, which delivers the values $s_{P,L}(v_j)$, $j = 1, \dots, K$, at arbitrary nodes in $\mathcal{O}(LP \log LP + K)$ operations.

All computations were performed in double precision on an Intel® Core™ i7-6700 CPU at 3.40 GHz, using Python 3.13 with NumPy 2.4 and the NFFT3 library [16] through its Python interface `pyNFFT3` 1.0.2 [26]. As a test function we use the two-sided exponential

$f(x) = \mathrm{e}^{-2\pi|x|}$ of Example 4.3 with $L = 8$, for which $\hat{f}(v) = \big(\pi(1+v^2)\big)^{-1}$ is known in closed form. Timings are the minimum over five runs after one warm-up run.

Table 5.1 compares the FFT with direct evaluation on the equispaced grid. Both compute the same quantity, and indeed they agree to machine precision; the FFT is faster by up to four orders of magnitude. The last column recalls the corresponding approximation error $M_{P,L}(f)$, which is the quantity bounded by Theorem 3.18. It is worth noting that the difference between the two algorithms is purely a matter of speed: the accuracy of the computed Fourier transform is governed entirely by $M_{P,L}(f)$ and not by the evaluation scheme.

Table 5.1: Equispaced output nodes $v = k/L$, $k \in [LP]$: direct evaluation versus FFT, for $f(x) = \mathrm{e}^{-2\pi|x|}$ and $L = 8$. The column $\|\cdot\|_\infty$ contains the maximum deviation between the two computed results.

P	LP	t_{direct} [s]	t_{FFT} [s]	speed-up	$\|\cdot\|_\infty$	$M_{P,L}(f)$
16	128	$8.0 \cdot 10^{-4}$	$4.2 \cdot 10^{-5}$	19	$1.7 \cdot 10^{-16}$	$2.55 \cdot 10^{-3}$
32	256	$3.2 \cdot 10^{-3}$	$4.7 \cdot 10^{-5}$	68	$2.5 \cdot 10^{-16}$	$6.43 \cdot 10^{-4}$
64	512	$1.2 \cdot 10^{-2}$	$5.8 \cdot 10^{-5}$	214	$2.2 \cdot 10^{-16}$	$1.61 \cdot 10^{-4}$
128	1024	$5.1 \cdot 10^{-2}$	$7.5 \cdot 10^{-5}$	683	$3.9 \cdot 10^{-16}$	$4.03 \cdot 10^{-5}$
256	2048	$2.1 \cdot 10^{-1}$	$1.1 \cdot 10^{-4}$	1853	$5.6 \cdot 10^{-16}$	$1.01 \cdot 10^{-5}$
512	4096	$9.0 \cdot 10^{-1}$	$1.8 \cdot 10^{-4}$	4895	$8.9 \cdot 10^{-16}$	$2.52 \cdot 10^{-6}$
1024	8192	$3.2 \cdot 10^{0}$	$3.5 \cdot 10^{-4}$	9271	$1.2 \cdot 10^{-15}$	$6.30 \cdot 10^{-7}$
2048	16384	$1.3 \cdot 10^{1}$	$6.9 \cdot 10^{-4}$	18355	$2.5 \cdot 10^{-15}$	$1.58 \cdot 10^{-7}$

The situation of real interest, however, is the evaluation at *arbitrary* nodes, where the FFT is not applicable at all. Table 5.2 compares the NFFT with direct evaluation at $K = 10\,000$ nodes drawn uniformly at random from $[-P/2, P/2)$. The NFFT is used with oversampling factor $\sigma = 2$ and cut-off parameter $m = 8$; the resulting relative deviation e_{NFFT} from the directly computed values stays at the level of the round-off error, while the speed-up reaches a factor of 4262 at $P = 4096$. The column $\max_j |\hat{f}(v_j) - s_{P,L}(v_j)|$ shows the error that is actually committed with respect to the true Fourier transform. It agrees with $\sqrt{L}\, M_{P,L}(f)$ to three digits in every row, i.e. the random nodes do attain the uniform bound. This illustrates once more that it is the *uniform* error (1.5), and not its discrete version (1.6), which governs the accuracy of the NFFT-based computation.

Finally, Table 5.3 documents step 4 of Algorithm 3.22, i.e. the choice of the NFFT cut-off parameter m. As predicted by [24, 25], the NFFT error decays exponentially in m, while the runtime grows only mildly. For $P = 256$ and $L = 8$ the approximation error is $\sqrt{L}\, M_{P,L}(f) = 2.85 \cdot 10^{-5}$, so that already $m = 3$ makes the NFFT error negligible; the frequently used default $m = 8$ reduces it to the level of round-off. In other words, the accuracy of the whole computation is determined by the parameters L and P through Theorem 3.5, and the NFFT contributes no relevant error at negligible additional cost.

Table 5.2: $K = 10\,000$ random nonequispaced nodes in $[-P/2, P/2)$: direct evaluation versus NFFT ($\sigma = 2$, $m = 8$), for $f(x) = \mathrm{e}^{-2\pi|x|}$ and $L = 8$. Here e_{NFFT} is the relative maximum deviation of the NFFT from the direct evaluation.

P	LP	t_{direct} [s]	t_{NFFT} [s]	speed-up	e_{NFFT}	$\max_j \lvert\hat{f}(v_j) - s_{P,L}(v_j)\rvert$
16	128	$7.2 \cdot 10^{-2}$	$1.50 \cdot 10^{-3}$	48	$3.8 \cdot 10^{-15}$	$7.22 \cdot 10^{-3}$
32	256	$1.3 \cdot 10^{-1}$	$1.52 \cdot 10^{-3}$	86	$3.7 \cdot 10^{-15}$	$1.82 \cdot 10^{-3}$
64	512	$2.6 \cdot 10^{-1}$	$1.56 \cdot 10^{-3}$	167	$4.2 \cdot 10^{-15}$	$4.56 \cdot 10^{-4}$
128	1024	$5.1 \cdot 10^{-1}$	$1.64 \cdot 10^{-3}$	310	$3.8 \cdot 10^{-15}$	$1.14 \cdot 10^{-4}$
256	2048	$1.0 \cdot 10^{0}$	$1.70 \cdot 10^{-3}$	586	$4.2 \cdot 10^{-15}$	$2.85 \cdot 10^{-5}$
512	4096	$2.0 \cdot 10^{0}$	$1.80 \cdot 10^{-3}$	1121	$3.8 \cdot 10^{-15}$	$7.13 \cdot 10^{-6}$
1024	8192	$4.0 \cdot 10^{0}$	$2.90 \cdot 10^{-3}$	1363	$4.5 \cdot 10^{-15}$	$1.78 \cdot 10^{-6}$
2048	16384	$7.7 \cdot 10^{0}$	$2.56 \cdot 10^{-3}$	3006	$9.4 \cdot 10^{-15}$	$4.45 \cdot 10^{-7}$
4096	32768	$1.6 \cdot 10^{1}$	$3.67 \cdot 10^{-3}$	4262	$2.4 \cdot 10^{-14}$	$1.11 \cdot 10^{-7}$

Table 5.3: Influence of the NFFT cut-off parameter m for $f(x) = \mathrm{e}^{-2\pi|x|}$, $P = 256$, $L = 8$, $K = 10\,000$ and $\sigma = 2$. For comparison, the approximation error of the sampling polynomial is $\sqrt{L}\, M_{P,L}(f) = 2.85 \cdot 10^{-5}$.

m	2	3	4	5	6	7	8
t_{NFFT} [ms]	1.6	2.1	1.6	1.6	1.6	1.6	1.7
e_{NFFT}	7.7e−5	8.7e−7	2.3e−8	1.5e−10	1.1e−12	1.8e−14	4.2e−15

6 Conclusion

We have studied how well the continuous Fourier transform $\hat{f}$ of an integrable function f can be approximated by the P-periodic trigonometric sampling polynomial $s_{P,L}$ of degree $LP/2$, measured in the uniform norm on the whole frequency interval $[-P/2, P/2]$.

The central result is Theorem 3.5, which bounds the scaled maximum approximation error $M_{P,L}(f)$ by the linear combination $L^{-1/2}\,\delta(\hat{f}, P) + L^{1/2}\,\delta(f, L)$ of the decay rates (3.2) of $\hat{f}$ and f. Combined with the explicit estimates of the decay rates in Lemma 3.9 and Lemma 3.15, this yields fully explicit error bounds under polynomial, exponential and mixed decay assumptions (Theorems 3.10, 3.16 and 3.18), in which every constant is determined by the decay parameters of f and $\hat{f}$. Theorem 3.20 shows that the resulting rate in the truncation parameter L is sharp.

These estimates have two consequences of practical importance. First, they can be used a priori: given a target accuracy, the parameters L and P can be determined before the computation is started, which is what Algorithm 3.22 does. Second, since the bound is uniform in v, it remains valid when $s_{P,L}$ is evaluated at arbitrary nodes by an NFFT. The NFFT thereby becomes a numerical method for the Fourier transform itself and not merely a fast evaluation scheme for trigonometric polynomials.

Our results also clarify the relation to the work of M. Ehler, K. Gröchenig and A. Klotz [8]. The scaled maximum error and the scaled Euclidean error are not equivalent; their quotient ranges over $[1, \sqrt{LP}\,]$, and both extremes occur (Remark 3.13). In the truncation dominated regime the two error measures agree up to a constant, whereas in the aliasing dominated regime the uniform estimate derived here is better by the factor $\sqrt{LP}$; Remark 3.12 traces this back to the different oscillatory behaviour of the aliasing

and the truncation remainder and explains why no symmetric bound can hold for the uniform error.

Acknowledgements

The authors would like to thank M. Ehler, K. Gröchenig, and H.G. Feichtinger for the fruitful discussions. They are further indebted to the reviewers for their careful reading of the manuscript and for their constructive comments, which lead in particular to the lower bound in Theorem 3.20, to the discussion of the time–frequency asymmetry in Remark 3.12 and Remark 3.13, and to the new Sections 2 and 5.

References

[1] T.M. Apostol. *Introduction to Analytic Number Theory.* Springer, New York, 1976.

[2] A.H. Barnett, J.F. Magland, and L. af Klinteberg, *A parallel nonuniform fast Fourier transform library based on an "exponential of semicircle" kernel*, SIAM J. Sci. Comput., 41 (2019), pp. C479–C504.

[3] A.H. Barnett, J.F. Magland, and L. af Klinteberg. Flatiron Institute nonuniform fast Fourier transform libraries (FINUFFT). `http://github.com/flatironinstitute/finufft`.

[4] A.H. Barnett. Aliasing error of the $\exp(\beta\sqrt{1-z^2})$ kernel in the nonuniform fast Fourier transform. *Appl. Comput. Harmon. Anal.*, 51:1–16, 2021.

[5] G. Beylkin. On the fast Fourier transform of functions with singularities. *Appl. Comput. Harmon. Anal.*, 2:363–381, 1995.

[6] W.L. Briggs and V.E. Henson. *The DFT. An Owner's Manual for the Discrete Fourier Transform.* SIAM, Philadelphia, 1995.

[7] A. Dutt and V. Rokhlin. Fast Fourier transforms for nonequispaced data. *SIAM J. Sci. Stat. Comput.*, 14:1368–1393, 1993.

[8] M. Ehler, K. Gröchenig, and A. Klotz. Quantitative estimates: How well does the discrete Fourier transform approximate the Fourier transform on $\mathbb{R}$? *SIAM Rev.* 68(1):93–123, 2026.

[9] H.G. Feichtinger. New results on regular and irregular sampling based on Wiener amalgams. *Function Spaces* (Edwardsville, IL, 1990), 107–121, Lecture Notes in Pure and Appl. Math., 136, Dekker, New York, 1992.

[10] M. Frigo and S. Johnson. The design and implementation of FFTW3. Proc. IEEE 93, 216–231, 2005.

[11] I.S. Gradstein and I.M. Ryshik. *Tables of Series, Products, and Integrals*. Vol. 1 and 2. Verlag Harri Deutsch, Thun, 1982.

[12] L. Greengard and J.-Y. Lee. Accelerating the nonuniform fast Fourier transform. *SIAM Rev.*, 46:443–454, 2004.

[13] K. Gröchenig. An uncertainty principle related to the Poisson summation formula. Studia Math. 121(1), 87–104, 1996.

[14] K. Gröchenig. *Foundations of Time–Frequency Analysis*. Birkhäuser, Boston, 2001.

[15] Y. Katznelson. Une remarque concernant la formula de Poisson. Studia Math. 29, 107–108, 1967.

[16] J. Keiner, S. Kunis, and D. Potts. NFFT 3.5, C subroutine library. `http://www.tu-chemnitz.de/~potts/nfft`. Contributors: F. Bartel, M. Fenn, T. Görner, M. Kircheis, T. Knopp, M. Quellmalz, M. Schmischke, T. Volkmer, A. Vollrath.

[17] J. Keiner, S. Kunis, and D. Potts. Using NFFT3 - a software library for various nonequispaced fast Fourier transforms. *ACM Trans. Math. Software*, 36:Article 19, 1–30, 2009.

[18] M. Kircheis, D. Potts, and M. Tasche. On regularized Shannon sampling formulas with localized sampling. *Sampl. Theory Signal Process. Data Anal.*, 20(20):34 pp., 2022.

[19] M. Kircheis, D. Potts, and M. Tasche. On numerical realizations of Shannon's sampling theorem. *Sampl. Theory Signal Process. Data Anal.*, 22(13):33 pp., 2024.

[20] M. Kircheis, D. Potts, and M. Tasche. Nonuniform fast Fourier transforms with nonequispaced spatial and frequency data and fast sinc transforms. *Numer. Algorithms*, 92:2307–2339, 2023.

[21] F. Oberhettinger. *Tables of Fourier Transforms and Fourier Transforms of Distributions*. Springer, Berlin, 1990.

[22] I. Pinelis. Exact lower and upper bounds on the incomplete gamma function. *Math. Inequal. Appl.*, 23(4): 1261–1278, 2020.

[23] G. Plonka, D. Potts, G. Steidl, and M. Tasche. *Numerical Fourier Analysis*. Applied and Numerical Harmonic Analysis. Birkhäuser/Springer, Second edition, 2023.

[24] D. Potts and M. Tasche. Uniform error estimates for nonequispaced fast Fourier transforms. *Sampl. Theory Signal Process. Data Anal.*, 19(17):1–42, 2021.

[25] D. Potts and M. Tasche. Continuous window functions for NFFT. *Adv. Comput. Math.*, 47:Article 53, 2021.

[26] pyNFFT3 – *Python interface for the* NFFT C *library*, Version 1.0.2, 2025. `https://github.com/NFFT/pyNFFT3`.

[27] L. Qian. On the regularized Whittaker–Kotelnikov–Shannon sampling formula. *Proc. Amer. Math. Soc.*, 131(4):1169–1176, 2003.

[28] G. Steidl. A note on fast Fourier transforms for nonequispaced grids. *Adv. Comput. Math.*, 9:337–353, 1998.

[29] T. Strohmer and J. Tanner. Fast reconstruction methods for bandlimited functions from periodic nonuniform sampling. *SIAM J. Numer. Anal.*, 44(3):1071–1094, 2006.

[30] N. Wiener, *The Fourier Integral and Certain of its Applications*, Cambridge University Press, Cambridge, 1988.